Research Square

Preprints are preliminary reports that have not undergone peer review. They should not be considered conclusive, used to inform clinical practice, or referenced by the media as validated information.

Metadichol®, a Novel Nano Lipid Formulation that Inhibits SARS-COV-2 and a Multitude of Pathological Viruses in vitro

Palayakotai Raghavan (raghavan@nanorxinc.com)
NANORX Inc.

Research

Keywords: Coronavirus, SARS-COV-2, COVID-19, ACE2, TMPRSS2, VDR, Metadichol

Posted Date: December 16th, 2020

DOI: https://doi.org/10.21203/rs.3.rs-34021/v6

License: This work is licensed under a Creative Commons Attribution 4.0 International License.
Read Full License

Version of Record: A version of this preprint was published at BioMed Research International on January 15th, 2022. See the published version at https://doi.org/10.1155/2022/1558860.

EDITORIAL NOTE:

10 October, 2023 Editorial note (correction). This submission initially contained a declaration of no competing interests for this submitted work; however, the author has now provided a corrected competing interest declaration as follows: The author, PR Raghavan, is the CEO of Nanorx Inc., the manufacturer of the Metadichol® supplement mentioned in this work, and, as such, has professional and financial interests related to research outcomes of this supplement.

Abstract

New pathogenic virus outbreaks, occurring with increasing regularity, are leading us to explore novel approaches, which will reduce the reliance on time-consuming vaccine modes to halt the outbreaks. The requirement is to find a universal approach to disarm any new and as yet unknown viruses as they appear. A promising approach could be targeting lipid membranes, which are common to all viruses and bacteria.

The ongoing pandemic of severe acute respiratory syndrome-coronavirus 2 (SARS-COV-2) has reaffirmed the importance of interactions between components of the host cell plasma membrane and the virus envelope as a critical mechanism of infection. Metadichol®, a nano lipid emulsion, has been examined and shown to be a strong candidate to help stop the proliferation of SARS-COV-2.

Naturally derived substances, such as long-chain saturated lipid alcohols, reduce the infectivity of various types of viruses, including coronaviruses such as SARS-COV-2, by modifying lipid-dependent attachment to human host cells. SARS-COV-2 uses the receptor ACE2 for entry and the serine protease TMPRSS2 for S protein priming.

Metadichol®, a nano lipid formulation of long-chain alcohols, has been shown to inhibit TMPRSS2 (EC50 96 ng/ml). Compared to the inhibitor camostat mesylate (EC50 26000 ng/ml), it is 270 times more potent. Additionally, Metadichol® is also a extremely weak inhibitor of ACE2 at 31 µg/ml. Further a live virus assay in Caco2 cells, Metadichol® inhibited SARS-CoV-2 replication with an EC90 of 0.16 µg/ml.

Introduction

There is currently an increasing need for a broad-spectrum antimicrobial agent that could inactivate human pathogens, such as bacteria and viruses. Rapid resistance by microorganisms has propelled this approach to the development of focused drugs. The most recent trigger is the fear of a future pandemic caused by new, poorly studied virulent strains, such as the present SARS-COV-2.

Background information on SARS-COV-2

Severe acute respiratory syndrome coronavirus 2 (SARS-COV-2) (causative agent of COVID-19) is causing a pandemic[1] that has produced global havoc within a few months. Medically controlling a rapidly spreading viral pandemic utilizing specific antivirals and vaccines will prove expensive and time consuming and is accompanied by compromises on safety and efficacy. An alternative approach is to test molecules that are already proven safe for effectiveness against SARS-COV-2. Among the candidates being tested are camostat mesylate (a 35-year-old Japanese drug), Avigan (another Japanese drug) and Gilead Science Inc.'s remdesivir[2].

To enter a host cell, SARS-COV-2 requires transmembrane protease serine 2 (TMPRSS2)[3], a serine protease, and angiotensin-converting enzyme 2 (ACE2)[4] to bind and thus facilitate its entry. Blocking both

receptors can effectively stop the cell entry mechanism used by the virus.

TMPRSS2 is a protease that primes the spike protein of SARS-COV and the Middle East respiratory syndrome-related coronavirus (MERS-COV). Camostat mesylate (CM), an inhibitor of TMPRSS2, inhibited SARS-COV in a mouse model[5,6]. Hoffmann et al.[7] determined that SARS-COV-2 requires TMPRSS2. They showed that CM blocks virus entry into the lungs. To date, there are no clinical data on the use of CM in patients.

The other receptor used by viruses to enter the host cell is ACE2. SARS-COV-2 has a spike (S) protein on its viral envelope (exterior) that binds to the transmembrane protein ACE2, which is present on human cells. ACE2 is essential for viral entry. However, ACE2 also regulates blood pressure and blood volume; blocking ACE2 would be detrimental to health. An approach that partially regulates ACE2 in concert with inhibition of TMPRSS2 would thus be an ideal solution.

Lipids and viruses

Viral envelope lipids play a role in both viral stability and infective capabilities. For example, substances that affect the lipid envelope, such as phospholipases, organic solvents, and surfactants, such as soaps, have been shown to affect viral infectivity. Causing envelope disintegration, they stop virus transmission to a new host. Active ingredients[8] in a number of cleaning agents, wipes, and tissues target the viral lipid envelope to render the virions nonviable. Snipes and coworkers[9] showed that saturated alcohols could inactivate viruses with chain lengths from 10 to 14 carbons. Their studies established that inactivation of enveloped viruses by lipids varies greatly, depending on both the nature of the lipid and the type of virus. Hilmarsson et al.[10-12] studied the virucidal effects of medium- and long-chain (8 to 18 carbon) fatty alcohols and corresponding lipids against herpes simplex viruses (HSV-1 and HSV-2), respiratory syncytial virus (RSV), human parainfluenza virus type 2 (HPIV2) and enveloped viruses at various concentrations, times and pH levels. After a 10-minute incubation at 37 °C with a 10 mM concentration, 14 of the lipids tested caused a 100000-fold or more significant reduction in HSV titre. Testing between pH 7 and 4.2 showed that a pH of 4.2 caused a more rapid inactivation of HSV-1 virus titre in one minute than higher pH values. These long-chain alcohols may act by penetrating the envelope of the virus by hydrophobic effects, making it permeable to small molecules and thus inactivating the virus; the degree of penetration into lipid membranes is based on the chain length of a lipid compared with the thickness of the membrane[13].

Metadichol ® is a nano lipid formulation of long-chain alcohols[14]. Metadichol has been shown to inhibit viruses in vitro and in vivo[15-17]. Metadichol was tested for its inhibitory actions against ACE2 and TMPRSS2 and in an antiviral assay with SARS-COV-2.

Discussion

The results in Table 1 and 2 demonstrate Metadichol's direct antiviral effect against the SARS-COV-2 virus in Caco-2 cells, with an EC90 of 0.15 µg/ml. Comparatively, this result indicates that Metadichol has a 2000-fold higher effectiveness than Remdesivir and 4000-fold potency over hydroxychloroquine phosphate[18].

A previously published work[15] of antiviral data against other viruses is shown in Tables 3 and 4. Raw data show the cytotoxicity of Metadichol without a virus present in Vero cells was measured by neutral red assay. When >75% "toxicity" occurred in the absence of virus, no viral CPE value was reported.

These results suggest that it is toxic to cells at concentrations above 5 ug/ml in most cases. However, Metadichol is not toxic, as the LD50 is 5000 mg/kg[19-21]. It is likely that Metadichol at higher concentrations behaves in a soap-mimicking manner by disrupting the lipid membrane, and at lower concentrations, it neutralizes the virus by a different mechanism. Metadichol is not toxic to cell lines, but rather, it behaves as a "detergent" in neutralizing SARS-COV-2 and other pathogenic viruses shown in Table 5. Additionally, Metadichol® targets selectively cancer cells in this case Caco-2 cells. In a previous study[22]of Klotho gene expression in the cancer cell lines Mia-Paca, Colo 205, and Panc1, Metadichol was seen to be toxic to cell lines above 1 µg/ml. It is also toxic at 10 µg/ml in leukaemia cancer cells[24]3

Metadichol also inhibits TMPRSS2 (Table 6 figure 1,2) and is 270-fold more potent than CM[24] Metadichol moderately inhibits ACE2 (Table 7, figures 3 and 4) and, in combination with TMPRSS2 inhibition, likely leads to a pronounced synergistic effect in overcoming viral entry. The reported results open the gateway to effective and safe therapies for COVID-19. Metadichol is a mild inhibitor of ACE2 (table 7 and figures 4 and 6) but at the same time, not significant to affect the physiological functions of the host.

Vitamin D and SARS-COV-2 infection

An uncontrolled inflammatory response to SARS-COV-2 is the major cause of disease severity and death in patients with COVID-19[25] and is associated with high levels of circulating cytokines, tumor necrosis factor (TNF), CCl2, C-reactive protein (CRP), and Ferritin. Metadichol[14] is an inhibitor of CCl2 (also known as MCP-1), TNF, NF-kB, and CRP, which is a surrogate marker for cytokine storms[26] and is associated with vitamin D deficiency.

Vitamin D3 is generated in the skin through the action of UVB radiation, with 7-dehydrocholesterol generated in the skin, followed by a thermal reaction. Vitamin D3 is converted to 25(OH)D in the liver and then to 1,25(OH)2D (calcitriol) in the kidneys. Calcitriol binds to the nuclear vitamin D receptor (VDR); a DNA-binding protein interacts with regulatory sequences near target genes that participate genetically and epigenetically in the transcriptional output of genes needed for function[27]. Vitamin D reduces the risk of infections by mechanisms that include inducing cathelicidins and defensins[28], resulting in lowered viral replication rates and reducing concentrations of pro-inflammatory cytokines[29]. Supplementation with 4000 IU/d vitamin D decreased dengue virus infection[30]. Inflammatory cytokine levels increase in

viral and bacterial infections, as seen in COVID-19 patients. Vitamin D can reduce the production of pro-inflammatory Th1 cytokines, such as TNF and interferon (IFN)[31].

Vitamin D is a modulator of adaptive immunity[32] and suppresses responses mediated by T helper type 1 (Th1) cells primarily by repressing the production of the inflammatory cytokines interleukin (IL)-2 and IFN-gamma[33]. Additionally, 1,25(OH)2D3 promotes cytokine production by T helper type 2 (Th2) cells, which helps enhance the indirect suppression of Th1 cells by complementing this suppression with actions mediated by a multitude of cell types[34].

1,25(OH)2D3 promotes T regulatory cell induction, thereby inhibiting inflammatory processes[35]. It is known that COVID-19 is associated with the increased production of pro-inflammatory cytokines, elevated CRP levels, increased risk of pneumonia, sepsis, acute respiratory distress syndrome (ARDS), and heart failure[36]. Case fatality rates (CFRs) in China were 6%-10% for those with cardiovascular disease, chronic respiratory tract disease, diabetes, and hypertension[37]. Metadichol is a inverse agonist/protean agonist [14] of VDR ie it binds at the same site as calcitriol but has different properties. It is the only known inverse agonist to VDR known in medical literature.

Telomerase and viral infections

Metadichol at one picogram increases h-TERT (telomerase) expression by 16-fold[38]. Viral infection places a significant strain on the body. CD8 T cells that mediate adaptive immunity[39] to protect the body from microbial invaders can easily reach their Hayflick limit by depleting their telomeres[40]. This possibility is more likely if telomeres are already short. Infections put enormous strain on immune cells to replicate. Naive T and B cells are particularly important when our bodies encounter new pathogens, such as SARS-COV-2. The quantity of these cells is crucial for useful immune function.

AHR and viral infections

One of the major issues with infected COVID-19 patients has been respiratory failure. It has been suggested that the aryl hydrocarbon receptor (AHR) is activated during coronavirus infections, impacting antiviral immunity and lung cells associated with repair[41]. Signalling via AHR may dampen the immune response against coronavirus[42]. It has been reported that although some signalling is needed for coronavirus replication, excessive activation of this pathway may be deleterious for the virus. AHR limits activation and interferes with multiple antiviral immune mechanisms, including IFN-I production and intrinsic immunity. Yamada et al.[43] suggested that AHR (the constitutive aryl hydrocarbon receptor) signalling constrains type I IFN-mediated antiviral innate defence and suggested a need to block constitutive AHR activity; only an inverse agonist can dampen this activity. We have shown that Metadichol® binds to AHR as an inverse/protean agonist[44] and thus can reduce complications attributed to uncontrolled inflammation and cytokine storms.

Vitamin C and viral infections

In infectious diseases, there is also a need to boost innate and adaptive immunity. The micronutrients with the most robust evidence for immune support are vitamins C and D. Vitamin C is essential for a healthy and functional host defence. The pharmacological application of vitamin C enhances immune function[45]. Vitamin C has antiviral properties leading to inhibition of the replication of HSV-1, poliovirus type 1, influenza virus type[46], and rabies virus in vitro[47].

Vitamin C deficiency reduces cellular[48-52]and humoral immune responses, and treatment of healthy subjects promoted and enhanced natural killer (NK) cell activities[53], underlining the immunological importance of vitamin C[54,55] and supporting its role as a crucial player in various aspects of immune cell functions, such as immune cell proliferation and differentiation, in addition to its anti-inflammatory properties. Moreover, the newly characterized hydroxylase enzymes, which regulate the activity of hypoxia-inducible factor gene transcription and cell signalling of immune cells, need vitamin C as a cofactor for optimal activity[56-58]. Metadichol administration increases vitamin C levels endogenously by recycling vitamin C and produces levels not reached by oral intake, and those reached bring about changes in improving diverse biomarkers[59-61].

Gene cluster network analysis

The present drug discovery paradigm is based on the idea of one gene-one target, one disease. It has become clear that it is difficult to achieve single target specificity. Thus, the need to transition from targeting a single gene to targeting multiple genes is likely to become more attractive, leading to blocking multiple paths of disease progression[62,63]. Gene network analysis can provide a minimum set of genes that can form the basis for targeting diseases. This clustering network of genes can modulate gene pathways and biological networks. We used www.ctdbase.org[64], which has curated genes show in Table 8 relevant to COVID-19. Table 9 lists genes and diseases states that they are involved in.

We can filter the 13 genes to a set of 5 genes: TNF, CCL2, ACE2, TMPRSS2 are modulated by Metadichol and AGT, which is part of the renin-angiotensin system (RAS) network that ACE2 is a part of (Figure 5). A similar analysis of these network genes shows that they are closely networked in diseases, with a highly significant p-value. These five genes are closely related, and the network generated, is shown in Figure 6, using www.innatedb.org[65]. This analysis integrates known interactions and pathways from major public databases.

The highlighted ones are SIRT1, AR (androgen receptor) , and FOS. Glinsky[66] suggested vitamin D as a potential mitigation agent in preventing SARS-COV-2 entry. Metadichol binds to VDR, which controls the expression of FOS[67]. AR also controls the expression of FOS, as well as that of TMPRSS2. Figure 7, generated below using PACO[68], shows the gene network and regulation relationships. VDR controls FOS expression, FOS controls AGT, AGT controls the expression of AGTR1 and ACE, and AR controls the expression of TMPRSS2.

Wambier and Goren[69] suggested that SARS-COV-2 infection is likely to be androgen mediated. The first step to infection is the priming of the SARS-COV-2 spike proteins by TMPRSS2, which also cleaves ACE2 for augmented viral entry. This pathway is seen in the network (Figure 8). SIRT1 plays an active role in enhancing immunity in viral infections[70]

Proteases such as Furin[71] and Adam-17 have been described to activate the spike protein in vitro for viral spread and pathogenesis in infected hosts. VDR controls Furin expression, mediated through its interaction with SRC[72]. Adam-17 is regulated via CEPBP[73,74], which is involved in the regulation of genes involved in immune and inflammatory responses. Recently, Ulrich and Pillat[75] proposed that CD147, similar to ACE2, is another receptor used for viral entry. CD147 is a known receptor[76] for the parasite that causes malaria in humans, *Plasmodium falciparum*. Metadichol (see Ref[6], US patent 9,006,292) inhibits the malarial parasite.

The key to entry into cells by SARS-COV-2 is ACE2, which, when endocytosed with SARS-COV-2, results in a reduction in ACE2 on cells and an increase in serum Angiostensin II[77]. Angiostensin II acts as a vasoconstrictor and a pro-inflammatory cytokine (Figure 9) via AT1R[78]. The Angiostensin II-AT1R axis leads to a pro-inflammatory state[79], leading to infections through activation of NF-KB and to increased IL-6 levels in multiple inflammatory and autoimmune diseases[80].

The dysregulation of angiotensin 2 downstream of ACE2 leads to the cytokine release that is seen in COVID-19 patients, resulting in increased TNF levels that lead to elevated IL-6, CCl2, and CRP levels. Cytokine storms[81] result in ARDS.

Controlling cytokine storms

A cytokine storm develops after an initial immune response by the induction of cytokines. The response to SARS-COV-2 leads to inflammation. There are increased levels of the pro-inflammatory cytokines IL-6, IL-18, TNF, and IL-1-beta by macrophages and of IFN-gamma by NK cells.

Figure 9 was generated, using of PACO (www.pathwcommons.org), shows the cytokine relationship network. The cytokines can activate T cells, which lead to tissue damage and infection in the lungs. Infiltration of T cells can also result from the upregulation of adhesion molecules, such as ICAM1, by lung endothelial cells. Metadichol is an inhibitor (see Ref[14], US patent 8,722,093) of TNF alpha in vivo, and ICAM1 and CCl2 depress the hyper inflammatory cytokine response caused by SARS-COV-2 and, at the same time, enhance innate and adaptive immunity through the VDR pathways and increased vitamin C levels. Metadichol, by its binding to VDR, leads to a network of gene control of the cytokine storms illustrated in Figure 6, bringing about homeostasis.

Clinical

A pilot study done by a third party Kasturaba Hospital in Mumbai India, on thirty COVID-19 patients with minor symptoms showed the absence of a virus in 75% of patients after 4 days of Metadichol treatment @ 20 mg per day. To validate this further, we have been initiated a larger study in collaboration with government agencies where we will have Metadichol treatment group and control groups, with only Standard Care. We hope to communicate these results in the near future.

Summary And Conclusions

Metadichol inhibits SARS-COV-2 entry into host cells by inhibiting TMPRSS2 and partial inhibition of ACE2 and boosts the antiviral response by enhancing innate and adaptive immunity through the vitamin D pathway and antiviral activity by endogenously increasing vitamin C levels. In addition, telomerase activity can also play a key role in maintaining the levels of naive T and B cells needed to fight infections. Metadichol modulates cytokine storms, as it is an inhibitor of TNF, ICAM1 and CCL2, which, as shown, play a key role with other cytokines. Co morbidities associated[82,83] with COVID-19, such as hypertension and diabetes[84,85], are also controlled by Metadichol, which could certainly improve the long-term prognosis for the affected patient population. These actions on multiple genes and via multiple pathways bring about homeostasis and prevent SARS-COV-2 infections. Metadichol's[86] actions on multiple genes and proteins lead to over 2000 unique interactions with other genes and result in a network that helps bring about homeostasis.

Metadichol is a safe, nontoxic product made from renewable sources and have been commercially available for the last six years, with no reported side effects. This unique property allows for the use of Metadichol as an immune modulator to prevent future occurrence of SARS-COV-2 and possibly other infections being predicted, facilitating a rapid return to normal human social and economic activity worldwide.

Abbreviations

Gene	Description
VDR	vitamin D receptor
AHR	aryl hydrocarbon receptor
TERT	telomerase reverse transcriptase
KL	klotho
PAI1 (SERPINE1)	serpin family E member 1
HIF 1 alpha	hypoxia-inducible factor 1-alpha
CCL2	C-C motif chemokine ligand 2
ICAM1	intercellular adhesion molecule 1
TNF	tumour necrosis factor
ACE	angiotensin I-converting enzyme
ACE2	angiotensin I-converting enzyme 2
AGTR1 (ANG1)	angiotensin II receptor type 1
AGTR2 (ANG2)	angiotensin II receptor type 2
TMPRSS2	transmembrane serine protease 2
SIRT1	sirtuin 1
TNF	tumour necrosis factor
FURIN	furin, paired basic amino acid cleaving enzyme
CD 147 (BSG)	Basigin (BSG), also known as extracellular matrix metalloproteinase inducer
IL6	interleukin 6
IL10	interleukin 10
CCL3	C-C motif chemokine ligand 3
IL2	interleukin 2
IL7	interleukin 7
CSF3	Colony-stimulating factor 3
IL2RA	interleukin 2 receptor subunit alpha
CXCL8	C-X-C motif chemokine ligand 8

Declarations

Competing interest: Author has no competing interests

Correspondence and requests for materials should be addressed to raghavan@nanorxinc.com

References

1. Morse, J. S., Lalonde, T., Xu, S. & Liu, W. R. Learning from the past: possible urgent prevention and treatment options for severe acute respiratory infections caused by 2019-nCoV. *Chembiochem* **21**, 730-738 (2020).
2. Li, G. & De Clercq, E. Therapeutic options for the 2019 novel coronavirus (2019-nCoV). *Nat. Rev. Drug Discov.* **19**, 149-150 (2020).
3. Jankun, J. COVID-19 pandemic; transmembrane protease serine 2 (TMPRSS2) inhibitors as potential drugs. *Translation* **7**, 1-5 (2020).
4. Hamming, I. et al. The emerging role of ACE2 in physiology and disease. *J. Pathol.* **212**, 1-11 (2007).
5. Rabaan, A. A. Middle East respiratory syndrome coronavirus: five years later. *Expert. Rev. Respir. Med.* **11**, 901-912 (2017).
6. Zhou, Y. et al. Protease inhibitors targeting coronavirus and filovirus entry. *Antivir. Res.* **116**, 76-84 (2015).
7. Hoffmann, M. et al. SARS- CoV-2 cell entry depends on ACE2 and TMPRSS2. A clinically proven protease inhibitor blocks it. *Cell* **181**, 271-280 (2020).
8. Greatorex, J. S. et al. Effectiveness of common household cleaning agents in reducing the viability of human influenza A/H1N1. *PLoS One* **5**, e8987 (2010).
9. Snipes, W., Person, S., Keller, G., Taylor, W. & Keith, A. Inactivation of lipid-containing viruses by long-chain alcohols. *Antimicrob. Agents Chemother.* **11**, 98-104 (1977).
10. Hilmarsson, H., Kristmundsdottir, T. & Thormar, H. Virucidal activities of medium- and long-chain fatty alcohols, fatty acids and monoglycerides against herpes simplex virus types 1 and 2: comparison at different pH levels. *APMIS* **113**, 58-65 (2005).
11. Hilmarsson, H., Larusson, L. V. & Thormar, H. Virucidal effect of lipids on visna virus, a lentivirus related to HIV. *Arch. Virol.* **151**, 1217-1224 (2006).
12. Hilmarsson, H., Traustason, B. S., Kristmundsdóttir, T. & Thormar, H. Virucidal activities of medium- and long-chain fatty alcohols and lipids against respiratory syncytial virus and parainfluenza virus type 2: comparison at different pH levels. *Arch. Virol.* **152**, 2225-2236 (2007).
13. Isaacs, C. E., Kims, K. & Thormar, H. Inactivation of enveloped viruses in human bodily fluids by purified lipids. *Ann. N. Y. Acad. Sci.* **724**, 457-464 (1994).
14. Raghavan, P. R. U.S patents 8,722, 094 (2014) ; 9,034,383 (2015) ; 9,006,292(2015).
15. Raghavan, P. R. In vitro inhibition of zika virus by Metadichol ®, a novel nano emulsion lipid. *J. Immunol. Tech. Infect. Dis.* **5**, 2-6 (2016).

16. Raghavan, P. R. Inhibition of Dengue and other enveloped viruses by Metadichol®, a novel Nanoemulsion Lipid. *J. Heal. Outcomes* **8**, 19-25 (2016).
17. Raghavan, P. R. Inhibition of viruses by Metadichol®: A novel nano emulsion lipid. *Pediatr. Infect. Dis.* **2**, 35 (2017).
18. Jin, Z., Du, X. & Yang, H. Structure of M^{pro} from SARS-CoV-2 and discovery of its inhibitors. *Nature* **582**, 289-293 (2020).
19. Aleman, C. et al. A 12-month study of policosanol oral toxicity in Sprague Dawley rats. *Toxicol. Lett.* **70**, 77-87 (1994).
20. Alemán, C. L. et al. Carcinogenicity of policosanol in sprague dawley rats: a 24 month study. *Teratog. Carcinog. Mutagen.* **14**, 239-249 (1994).
21. Alemán, C. L. et al. Carcinogenicity of policosanol in mice: an 18-month study. *Food Chem. Toxicol.* **33**, 573-578 (1995).
22. Raghavan, P. R. Metadichol® a novel agonist of the anti-aging klotho gene in cancer cell lines. *J. Cancer Sci. Ther.* **10**, 351-357 (2018)..
23. P. R. Raghavan unpublished results.
24. Uno, Y. Camostat mesilate therapy for COVID-19. Preprint at https://pubmed.ncbi.nlm.nih.gov/32347443 (2020).
25. Merad, M. & Martin, J. C. Pathological inflammation in patients with COVID-19: a key role for monocytes and macrophages. *Nat. Rev. Immunol.* **20**, 355-362 (2020).
26. Daneshkhah, A. et al. The possible role of Vitamin D in suppressing cytokine storm and associated mortality in COVID-19 patients. *medRxiv* **4**, 20058578 (2020).
27. Pike, J. W. & Christakos, S. Biology and mechanisms of action of the Vitamin D hormone. *Endocrinol. Metab. Clin. N. Am.* **46**, 815-843 (2017).
28. Liu, P. T. et al. Convergence of IL-1beta and VDR activation pathways in human TLR2/1-induced antimicrobial responses. *PLoS One* **4**, e5810 (2009).
29. Wang, T.-T. et al. Cutting edge: 1,25-dihydroxyvitamin D3 is a direct inducer of antimicrobial peptide gene expression. *J. Immunol.* **173**, 2909-2912 (2004).
30. Martínez-Moreno, J., Hernandez, J. C. & Urcuqui-Inchima, S. Effect of high doses of vitamin D supplementation on dengue virus replication, Toll-like receptor expression, and cytokine profiles on dendritic cells. *Mol. Cell Biochem.* **464**, 169-180 (2020).
31. Spilianakis, C. G., Lee, G. R. & Flavell, R. A. Twisting the Th1/Th2 immune response via the retinoid X receptor: lessons from a genetic approach. *Eur. J. Immunol.* **35**, 3400-3404 (2005).
32. Wei, R. & Christakos, S. Mechanisms underlying the regulation of innate and adaptive immunity by Vitamin D. *Nutrients* **7**, 8251-8260 (2015).
33. Cantorna, M. T., Snyder, L., Lin, Y.-D. & Yang, L. Vitamin D and 1,25(OH)2D regulation of T cells. *Nutrients* **7**, 3011-3021 (2015).

34. Cantorna, M. T. Mechanisms underlying the effect of vitamin D on the immune system. *Proc. Nutr. Soc.* **69**, 286-289 (2010).
35. Lemire, J. M. et al. 1,25-dihydroxyvitamin D3 suppresses human T helper/inducer lymphocyte activity in vitro. *J. Immunol.* **134**, 3032-3035 (1985).
36. Huang, C. et al. Clinical features of patients infected with 2019 novel coronavirus in Wuhan, China. *Lancet (London, England)* **395**, 497-506 (2020).
37. Wang, D. et al. Clinical characteristics of 138 hospitalized patients with 2019 novel coronavirus-infected pneumonia in Wuhan, China. *JAMA* **323**, 1061-1069 (2020).
38. Raghavan, P. R. Metadichol® and CD33 expression in umbilical cord cells. *J. Stem Cell Res. Ther.* **9**, 446 (2019).
39. Weng, N. P. Telomere and adaptive immunity. *Mech. Ageing Dev.* **129**, 60-66 (2008).
40. Hodes, R. J., Hathcock, K. S. & Weng, N. P. Telomeres in T and B cells. *Nat. Rev. Immunol.* **2**, 699-706 (2002).
41. Poppe, M. et al. The NF-κB-dependent and -independent transcriptome and chromatin landscapes of human coronavirus 229E-infected cells. *PLoS Pathog.* **13**, e1006286 (2017).
42. Giovannoni, F. et al. AHR is a Zika virus host factor and a candidate target for antiviral therapy. *Nat. Neurosci.* **22**, 729-740 (2019).
43. Yamada, T. et al. Constitutive aryl hydrocarbon receptor signaling constrains type I interferon–mediated antiviral innate defense. *Nat. Immunol.* **17**, 687-694 (2016).
44. Raghavan, P. R. Metadichol ®. A novel inverse agonist of aryl hydrocarbon receptor (AHR) and NRF2 inhibitor. *J. Cancer Sci. Ther.* **9**, 661-668 (2017).
45. Heuser, G. & Vojdani, A. Enhancement of natural killer cell activity and T and B cell function by buffered Vitamin C in patients exposed to toxic chemicals: the role of protein kinase-C. *Immunopharmacol. Immunotoxicol.* **19**, 291-312 (1997).
46. Furuya, A. et al. Antiviral effects of ascorbic and dehydroascorbic acids in vitro. *Int. J. Mol. Med.* **22**, 541-545 (2008).
47. Kim, H. et al. Red ginseng and vitamin C increase immune cell activity and decrease lung inflammation induced by influenza A virus/H1N1 infection. *J. Pharm. Pharmacol.* **68**, 406-420 (2016).
48. Madhusudana, S. N., Shamsundar, R. & Seetharaman, S. In vitro inactivation of the rabies virus by ascorbic acid. *Int. J. Infect. Dis.* **8**, 21-25 (2004).
49. Alvares, O., Altman, L. C., Springmeyer, S., Ensign, W. & Jacobson, K. The effect of subclinical ascorbate deficiency on periodontal health in nonhuman primates. *J. Periodontal. Res.* **16**, 628-636 (1981).
50. Goldschmidt, M. C., Masin, W. J., Brown, L. R. & Wyde, P. R. The effect of ascorbic acid deficiency on leukocyte phagocytosis and killing of actinomyces viscosus. *Int. J. Vitam. Nutr. Res.* **58**, 326-334 (1988).

51. Wintergerst, E. S., Maggini, S. & Hornig, D. H. Immune-enhancing role of Vitamin C and zinc and effect on clinical conditions. *Ann. Nutr. Metab.* **50**, 85-94 (2006).
52. Woo, A. et al. Vitamin C acts indirectly to modulate isotype switching in mouse B cells. *Anat. Cell Biol.* **43**, 25-35 (2010).
53. Carr, A. C. & Maggini, S. Vitamin C and immune function. *Nutrients* **9**, 1211 (2017).
54. Washko, P., Rotrosen, D. & Levine, M. Ascorbic acid in human neutrophils. *Am. J. Clin. Nutr.* **54**, 1221S-1227S (1991).
55. Kuiper, C. & Vissers, M. C. M. Ascorbate as a co-factor for fe- and 2-oxoglutarate dependent dioxygenases: physiological activity in tumor growth and progression. *Front. Oncol.* **4**, 359 (2014).
56. Loenarz, C. & Schofield, C. J. Physiological and biochemical aspects of hydroxylations and demethylations catalyzed by human 2-oxoglutarate oxygenases. *Trends Biochem. Sci.* **36**, 7-18 (2011).
57. Flashman, E., Davies, S. L., Yeoh, K. K. & Schofield, C. J. Investigating the dependence of the hypoxia-inducible factor hydroxylases (factor inhibiting HIF and prolyl hydroxylase domain 2) on ascorbate and other reducing agents. *Biochem. J.* **427**, 135-142 (2010).
58. Kuiper, C., Dachs, G. U., Currie, M. J. & Vissers, M. C. M. Intracellular ascorbate enhances hypoxia-inducible factor (HIF)-hydroxylase activity and preferentially suppresses the HIF-1 transcriptional response. *Free Radic. Biol. Med.* **69**, 308-317 (2014).
59. Raghavan, P. R. Metadichol®, Vitamin C and GULO gene expression in mouse adipocytes. *Biol. Med.* **10**, 426 (2017).
60. Raghavan, P. R. Metadichol® and Vitamin C increase in vivo, an open-label study. *Vitam. Miner.* **6**, 163 (2017).
61. Raghavan, P. R. Metadichol® induced high levels of Vitamin C: case studies. *Vitam. Miner.* **6**, 169 (2017).
62. Creixell, P. et al. Pathway and network analysis of cancer genomes. *Nat. Methods* **12**, 615-621 (2015).
63. Barabási, A.-L., Gulbahce, N. & Loscalzo, J. Network medicine: a network-based approach to human disease. *Nat. Rev. Genet.* **12**, 56-68 (2011).
64. Davis, A. P. et al. The comparative toxicogenomics database: update 2019. *Nucleic Acids Res.* **47**, D948-D954 (2019).
65. Breuer, K. et al. InnateDB: systems biology of innate immunity and beyond–recent updates and continuing curation. *Nucleic Acids Res.* **41**, D1228-D1233 (2013).
66. Glinsky, G. Genomics-guided molecular maps of coronavirus targets in human cells: a path toward the repurposing of existing drugs to mitigate the pandemic. arXiv:2003.13665 (2020).
67. Meyer, M. B., Goetsch, P. D. & Pike, J. W. VDR/RXR and TCF4/β-catenin cistromes in colonic cells of colorectal tumor origin: impact on c-FOS and c-MYC gene expression. *Mol. Endocrinol.* **26**, 37-51 (2012).

68. Rodchenkov, I. et al. Pathway commons 2019 update: integration, analysis and exploration of pathway data. *Nucleic Acids Res.* **48**, D489-D497 (2020).
69. Wambier, C. G. & Goren, A. Severe acute respiratory syndrome coronavirus 2 (SARS-CoV-2) infection is likely to be androgen mediated. *J. Am. Acad. Dermatol.* **83**, 308-309 (2020).
70. Lin, Z. & et al. Sirt involvement in virus-mediated diseases. *JSM Microbiol.* **1**, 1006 (2013).
71. Ma, Y. C. et al. The tyrosine kinase c-Src directly mediates growth factor-induced Notch-1 and Furin interaction and Notch-1 activation in pancreatic cancer cells. *PLoS One* **7**, e33414 (2012).
72. Buitrago, C., Vazquez, G., De Boland, A. R. & Boland, R. L. Activation of Src kinase in skeletal muscle cells by 1,25-(OH)2-vitamin D3 correlates with tyrosine phosphorylation of the vitamin D receptor (VDR) and VDR-Src interaction. *J. Cell. Biochem.* **79**, 274-281 (2000).
73. Marchwicka, A. & Marcinkowska, E. Regulation of expression of CEBP genes by variably expressed Vitamin D receptor and retinoic acid receptor α in human acute myeloid leukemia cell lines. *Int. J. Mol. Sci.* **19**, 1918 (2018).
74. Arcidiacono, M. V., Yang, J., Fernandez, E. & Dusso, A. The induction of C/EBPβ contributes to vitamin D inhibition of ADAM17 expression and parathyroid hyperplasia in kidney disease. *Nephrol. Dial. Transplant.* **30**, 423-433 (2015).
75. Ulrich, H. & Pillat, M. M. CD147 as a target for COVID-19 treatment: suggested effects of azithromycin and stem cell engagement. *Stem. Cell Rev. Rep.* **16**, 434-440 (2020).
76. Crosnier, C. et al. Basigin is a receptor essential for erythrocyte invasion by Plasmodium falciparum. *Nature* **480**, 534-537 (2011).
77. Kuba, K. et al. A crucial role of angiotensin converting enzyme 2 (ACE2) in SARS coronavirus-induced lung injury. *Nat. Med.* **11**, 875-879 (2005).
78. Eguchi, S., Kawai, T., Scalia, R. & Rizzo, V. Understanding angiotensin II type 1 receptor signaling in vascular pathophysiology. *Hypertension* **71**, 804-810 (2018).
79. Murakami, M., Kamimura, D. & Hirano, T. Pleiotropy and specificity: insights from the interleukin 6 family of cytokines. *Immunity* **50**, 812-831 (2019).
80. de Wit, E., van Doremalen, N., Falzarano, D. & Munster, V. J. SARS and MERS: recent insights into emerging coronaviruses. *Nat. Rev. Microbiol.* **14**, 523-534 (2016).
81. Pedersen, S. F. & Ho, Y.-C. SARS-CoV-2: a storm is raging. *J. Clin. Investig.* **130**, 2202-2205 (2020).
82. Guo, W. et al. Diabetes is a risk factor for the progression and prognosis of COVID-19. *Diabetes/Metab. Res. Rev.* **202**, e3319 (2020).
83. Wu, C. et al. Risk factors associated with acute respiratory distress syndrome and death in patients with coronavirus disease 2019 pneumonia in Wuhan, China. *JAMA Intern. Med.* **13**, e200994 (2020).
84. Raghavan, P. R. Systolic and diastolic BP control in metabolic syndrome patients with Metadichol® a novel nano emulsion lipid. *J. Cardiol. Cardiovasc. Ther.* **5**, 555660 (2017).
85. Raghavan, P. R. Metadichol and type 2 diabetes a case report. *J. Sci. Heal Outcomes* **8**, 5-10 (2106).
86. Raghavan, P. R. https://www.researchgate.net/profile/Palayakotai_Raghavan/publications.

Methods

All assays were on a fee-for-service contract basis and outsourced to bioanalytical testing companies worldwide. SARS-COV-2 antiviral assays were performed by a bio-safety level 3 (BSL3) facility at the Antiviral research Institute at Utah State University in the USA. The other assays were performed at Southern Research Infectious Disease Research Facility in Frederick, Maryland, USA and IBT Bio services in Rockville, Maryland, USA. ACE2 and TMPRSS2 Assays were carried out by Skanda Life Sciences Pvt Ltd Bangalore , India.

Antiviral assay

Metadichol was serially diluted using eight half-log dilutions in test medium (MEM supplemented with 2% FBS and 50 µg/mL gentamicin) so that the starting (high) test concentration was 100 µg/ml. Each dilution was added to 5 wells of a 96-well plate with 80-100% confluent Caco-2 cells.

Three wells of each dilution were inoculated with virus, with two wells uninoculated (as toxicity controls); six wells were inoculated and untreated (as virus controls); and six wells were uninoculated and untreated (as cell controls). SARS-COV-2 was prepared to achieve the lowest possible multiplicity of infection (MOI) that would yield >80% cytopathic effect (CPE) within five days. M128533 (protease specific for SARS-COV) was tested in parallel as a positive control. The plates were incubated at 37±2°C and 5% CO_2. On day three post-infection, once untreated virus control wells reached maximum CPE, plates were stained with neutral red dye for approximately 2 hours (±15 minutes). The supernatant dye was removed, and the wells were rinsed with PBS. The incorporated dye was extracted in 50:50 Sorensen citrate buffer/ethanol for >30 minutes, and the optical density was read on a spectrophotometer at 540 nm.

Optical densities were converted to percent of that of cell controls, and the concentration of compound that would cause 50% cell death (CC50) in the absence of virus was calculated by regression analysis. The selective index (SI) is the CC50 divided by the EC90. The results are shown in Table 7.

For a virus yield reduction (VYR) assay, the supernatant fluid from each compound concentration was collected on day three post-infection before neutral red staining (3 wells pooled) and tested for virus titre using a standard endpoint dilution CCID50 assay in Vero 76 cells and titre calculations via the Reed-Muench (1948) equation. The concentration of compound required to reduce virus yield by one log10 was calculated by regression analysis (EC90).

As shown in Table 2 the virus reduction assay did not follow a typical dose-response relationship, with virus reduction seen at concentrations of 0.3 µg/ml and 3.2 µg/ml but no reduction seen at a concentration of 1 µg/ml. It was assumed that breakthrough of the virus at 1 µg/ml was an outlier. The calculated SI was 20 (Table 1), indicating an EC90 of 0.15 µg/ml.

The results for other viruses shown in Table 3 and 4 and 5 were carried out in a similar procedure by various labs using Vero cells.

TMPRSS2 inhibition assay

Procedure

TMPRSS purified from LNCaP cells (ATCC) was used as an enzyme source. The reaction mixture contained purified TMPRSS2 protease in TBS with or without a range of various concentrations from 1.56 to 100 ng/ml of test sample or inhibitor. The reaction mixture was incubated for 10 minutes at 37°C. To the reaction mixture, 1 µl of 10 mM the fluorogenic trypsin substrate Cbz-Gly-Gly-Arg-AMC was added, and kinetic fluorescence readings were recorded after 2 minutes of incubation at 37°C at Ex383 nm and Em455 nm at 5-10 minutes using a SpectraMax i3X (Molecular Devices). The change in fluorescence (delta RFU) was calculated to determine the inhibitory effects of the test sample. CM (Cayman Chemicals) at a two-fold range of concentrations from 1.56 to 100 nM was used as a positive control for TMPRSS2 protease inhibition.

ACE2 Inhibition assay

An ACE2 Inhibitor Screening Assay Kit, catalogue no. 79923 (BPS Biosciences, San Diego, USA), was used to measure the exopeptidase activity of ACE2 and inhibition by Metadichol and the control inhibitor DX600. The inhibitory activity was measured based on the fluorescence emitted by the cleavage of a chromogenic substrate.

Procedure

Enzyme (ACE2) stocks were prepared from the supplied kit. Twenty micro litres of enzyme solution (0.5 ng/µl) was added to all the wells designated for the assay. DX600, a potent ACE2 inhibitor, was used as a positive control for ACE2 inhibition at various concentrations ranging from 0.0156 µg/ml to 1 µg/ml. The test sample at concentrations ranging from 0.125 µg/ml to 40 µg/ml was used. To each well containing the enzyme solution, 5 µl of inhibitor solution was added to the respective designated wells. The reaction mixture was incubated at room temperature for 5 minutes. After incubation, 25 µl of ACE2 substrate was added to the mixture and incubated for 1 hour at room temperature. The RFU due to cleavage of the substrate were read at Ex555 nm and Em585 nm using a SpectraMax i3x (Molecular Devices). The IC50 values were calculated based on the readings obtained.

Tables

Table 1. In vitro antiviral assay results

	CC50	EC90	SI90
Metadichol (µg/ml)	4	0.15	20
M128533 (µg/ml)	>10	0.2	>33

CC50: 50% cytotoxic concentration of compound without virus added;

EC50: 50% effective antiviral concentration;

EC90: calculated concentration to reduce virus yield by 1 log (90%);

SI: CC50/EC50.

Table 2. Cytotoxicity and virus yield data for each concentration of Metadichol tested

Metadichol Concentration (µg/ml)	Cytotoxicity (%)	Virus Titre (CCID50 per 0.1 ml)
100	100%	<0.7
32	100%	<0.7
10	83%	<0.7
3.2	54%	0.7
1	17%	4.3
0.3	26%	1.5
0.1	26%	5.7
0.03	26%	5.3

Table 3. Raw data for cytotoxicity of Metadichol without virus present, as measured by neutral red assay

Units are µg/ml unless noted								
Metadichol (µg/ml)	Adenovirus	Tacaribe	Rift valley	SARS	Japanese encephalitis	West Nile virus	Yellow fever	Powassan virus
500	95%	98%	96%	96%	100%	100%	100%	100%
160	92%	98%	96%	95%	100%	100%	100%	100%
50	90%	97%	97%	95%	100%	100%	100%	100%
16	85%	95%	81%	92%	88%	77%	98%	100%
5	0%	23%	26%	35%	33%	28%	35%	44%
1.6	0%	2%	10%	15%	12%	14%	19%	6%
0.5	0%	3%	9%	0%	2%	3%	2%	0%
0.16	0%	17%	3%	0%	0%	0%	4%	0%
CC50	9.90	7.30	8.40	6.70	7.20	8.50	5.00	5.1

Table 4 Antiviral assay of Metadichol against various viruses, as measured by neutral red assay

Metadichol (µg/ml)	Adenovirus	Tacaribe	Rift valley fever	SARS	Japanese encephalitis	West Nile	Yellow fever	Powassan
5	100%	31%	100%	0%	56%	84%	70%	53%
1.6	100%	69%	100%	52%	87%	100%	73%	100%
0.5	100%	97%	100%	100%	100%	100%	95%	100%
0.16	100%	100%	100%	100%	100%	100%	96%	100%
EC50	>9.9	2.8	>8.4	1.7	>7.2	>8.5	>5	>5.1

Table 5. List of viruses inhibited by Metadichol in vitro

Adenovirus	Rift valley
Japanese encephalitis	Marburg
Tacaribe	SARS
Powassan	Respiratory syncytial virus
Zika	Chikungunya
Ebola	Influenza A (H1N1)
Yellow fever	Dengue
West Nile virus	HIV

Table 6. TMPRSS2 assay data

Sample	Concentration	RFU	% Inhibition	IC50
Control	0	43233358	0.00	
Metadichol (ng/ml)	1.56	41305150	4.46	96.65 ng/ml
	3.12	39329385	9.03	
	6.25	36713767	15.08	
	12.5	33778222	21.87	
	25	30695684	29.00	
	50	26087008	39.66	
	100	16009312	62.97	
Camostat mesylate (µg/ml)	0.78	37984828	12.14	26.46 ug/ml
	1.56	35235186	18.50	
	3.125	31685728	26.71	
	6.25	29234396	32.38	
	12.5	23276839	46.16	
	25	18931887	56.21	
	50	8797988	79.65	

Table 7 ACE2 assay data

Sample	Concentration (µg/ml)	RFU	% Inhibition	IC50 (µg/ml)
Control	0	308315546	0.00	
Metadichol	0.125	290309918	5.84	30.15
	0.25	260064163	15.65	
	0.5	249149792	19.19	
	1	240301136	22.06	
	10	212275253	31.15	
	20	187702504	39.12	
	40	139821100	54.65	
DX600	0.0156	252855648	17.99	0.1027
	0.031	231028864	25.07	
	0.0625	193810784	37.14	
	0.125	145881248	52.68	
	0.25	127485752	58.65	
	0.5	111498760	63.84	

Table 8. COVID-19 and 13 curated genes

CCL2	IL6	IL7
TNF	TMPRSS2	ACE2
IL10	CCL3	AGT
IL2	IL8	IL2RA
CSF3		

Table 9. Disease network of the 13 curated genes

Disease name	Disease categories	Corrected P-value	Annotated gene quantity	Annotated genes
COVID-19	Respiratory tract disease, viral disease	3.10E-47	13	ACE2, AGT, CCL2, CCL3, CSF3, CXCL10, IL10, IL2, IL2RA, IL6, IL7, TMPRSS2, TNF
Pneumonia, viral	Respiratory tract disease, viral disease	4.34E-46	13	ACE2, AGT, CCL2, CCL3, CSF3, CXCL10, IL10, IL2, IL2RA, IL6, IL7, TMPRSS2, TNF
Coronaviridae infections	Viral disease	1.74E-44	13	ACE2, AGT, CCL2, CCL3, CSF3, CXCL10, IL10, IL2, IL2RA, IL6, IL7, TMPRSS2, TNF
Coronavirus infections	Viral disease	1.74E-44	13	ACE2, AGT, CCL2, CCL3, CSF3, CXCL10, IL10, IL2, IL2RA, IL6, IL7, TMPRSS2, TNF
Nidovirales infections	Viral disease	1.74E-44	13	ACE2, AGT, CCL2, CCL3, CSF3, CXCL10, IL10, IL2, IL2RA, IL6, IL7, TMPRSS2, TNF
RNA virus infections	Viral disease	4.92E-27	13	ACE2, AGT, CCL2, CCL3, CSF3, CXCL10, IL10, IL2, IL2RA, IL6, IL7, TMPRSS2, TNF
Virus diseases	Viral disease	1.73E-25	13	ACE2, AGT, CCL2, CCL3, CSF3, CXCL10, IL10, IL2, IL2RA, IL6, IL7, TMPRSS2, TNF
Sexually transmitted diseases, viral	Viral disease	1.38E-12	7	CCL2, CCL3, IL10, IL2, IL2RA, IL6, TNF
HIV infections	Immune system disease, viral disease	1.56E-12	7	CCL2, CCL3, IL10, IL2, IL2RA, IL6, TNF
Lentivirus infections	Viral disease	1.56E-12	7	CCL2, CCL3, IL10, IL2, IL2RA, IL6, TNF
Retroviridae infections	Viral disease	1.56E-12	7	CCL2, CCL3, IL10, IL2, IL2RA, IL6, TNF
HIV wasting syndrome	Immune system disease, metabolic disease, nutrition disorder, viral disease	4.00E-04	2	IL6, TNF
Coxsackievirus infections	Viral disease	0.001	2	IL6, TNF
Enterovirus infections	Viral disease	0.0044	2	IL6, TNF
Picornaviridae infections	Viral disease	0.00519	2	IL6, TNF

Table 10. Disease network of genes implicated in SARS-COV-2 infection

Disease name	P-value	Corrected P-value	Genes	Annotated genes
COVID-19	1E-18	5.44E-16	5	ACE2, AGT, CCL2, TMPRSS2, TNF
Pneumonia, viral	1.56E-18	8.46E-16	5	ACE2, AGT, CCL2, TMPRSS2, TNF
Coronaviridae infections	3.4E-18	1.85E-15	5	ACE2, AGT, CCL2, TMPRSS2, TNF
Coronavirus infections	3.4E-18	1.85E-15	5	ACE2, AGT, CCL2, TMPRSS2, TNF
Nidovirales infections	3.4E-18	1.85E-15	5	ACE2, AGT, CCL2, TMPRSS2, TNF
Pneumonia	9.42E-15	5.11E-12	5	ACE2, AGT, CCL2, TMPRSS2, TNF
Respiratory tract infections	3.13E-13	1.7E-10	5	ACE2, AGT, CCL2, TMPRSS2, TNF
RNA virus infections	2.46E-12	1.34E-09	5	ACE2, AGT, CCL2, TMPRSS2, TNF
Virus diseases	9.48E-12	5.15E-09	5	ACE2, AGT, CCL2, TMPRSS2, TNF

Figures

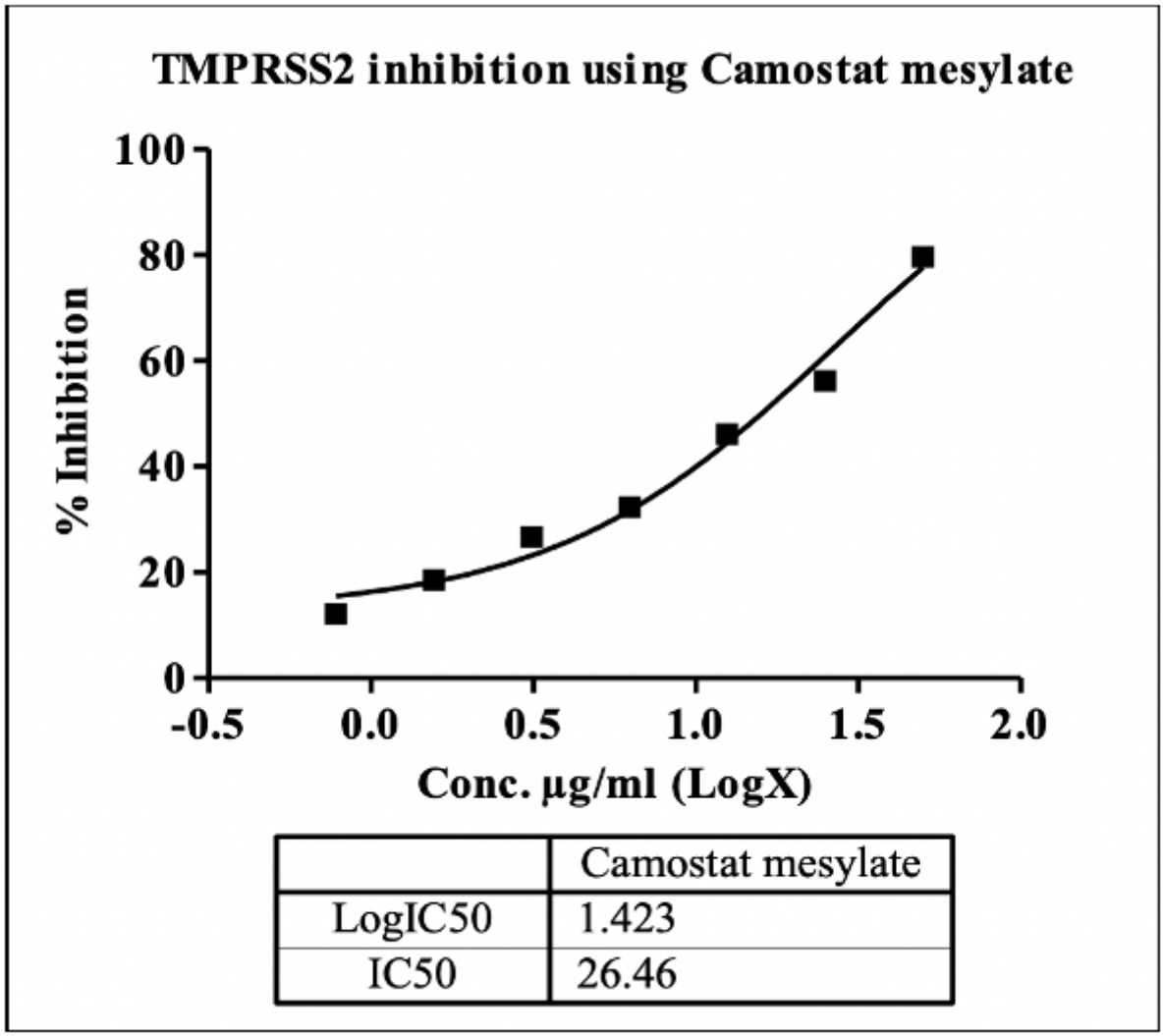

	Camostat mesylate
LogIC50	1.423
IC50	26.46

Figure 1

TMPRSS2 inhibition with Camostat mesylate (control)

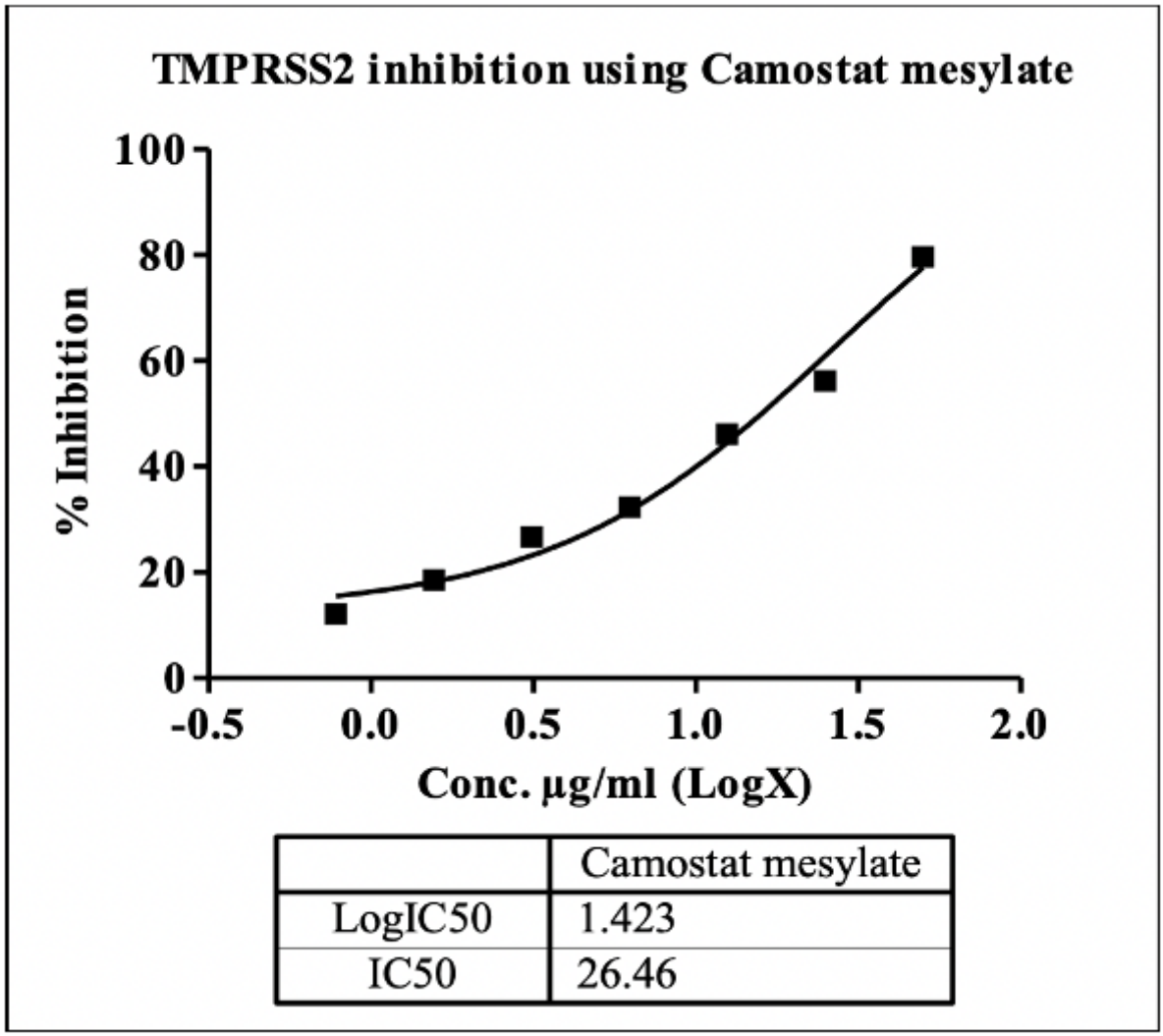

	Camostat mesylate
LogIC50	1.423
IC50	26.46

Figure 1

TMPRSS2 inhibition with Camostat mesylate (control)

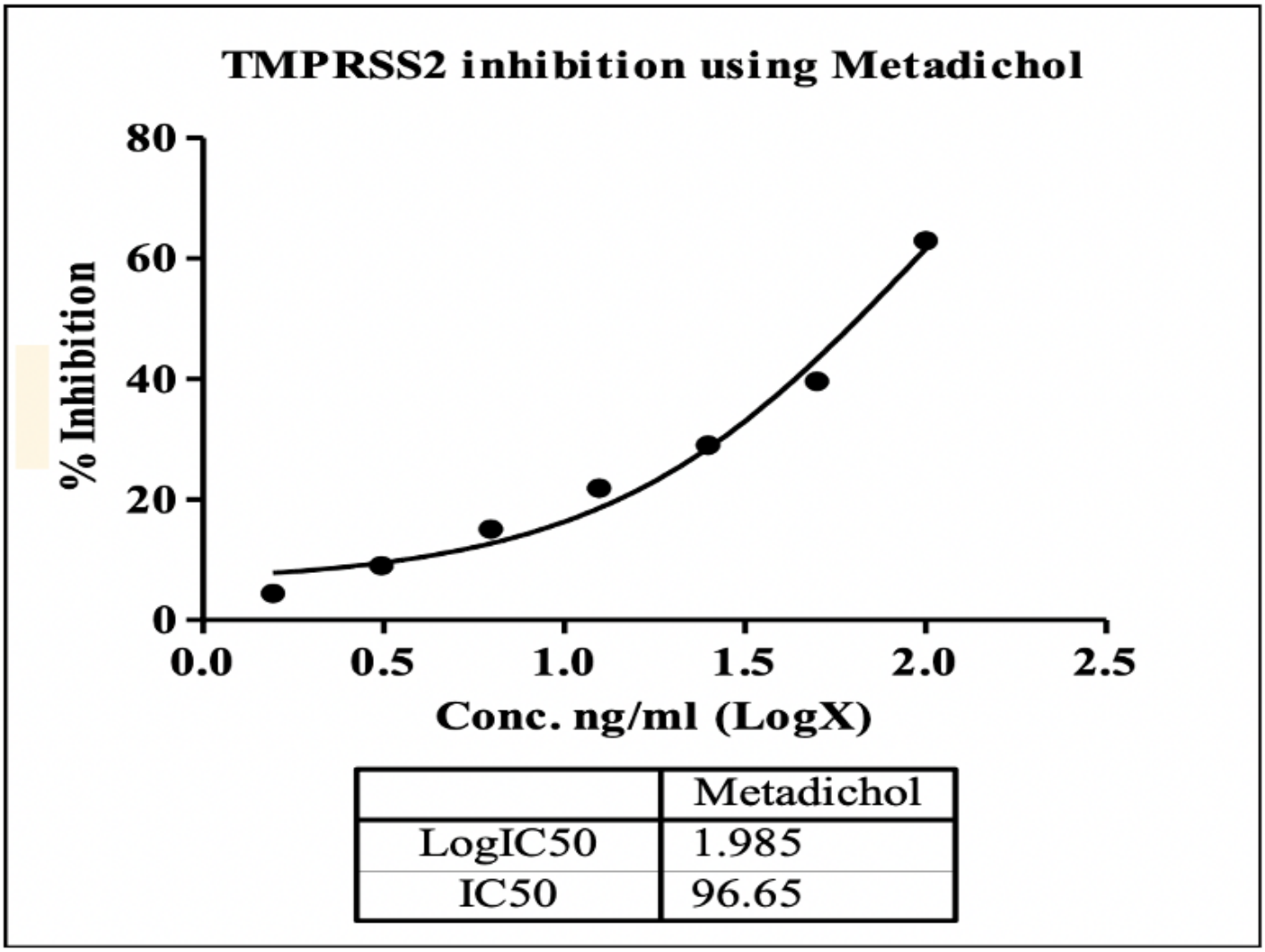

Figure 2

TMPRSS2 inhibition with Metadichol

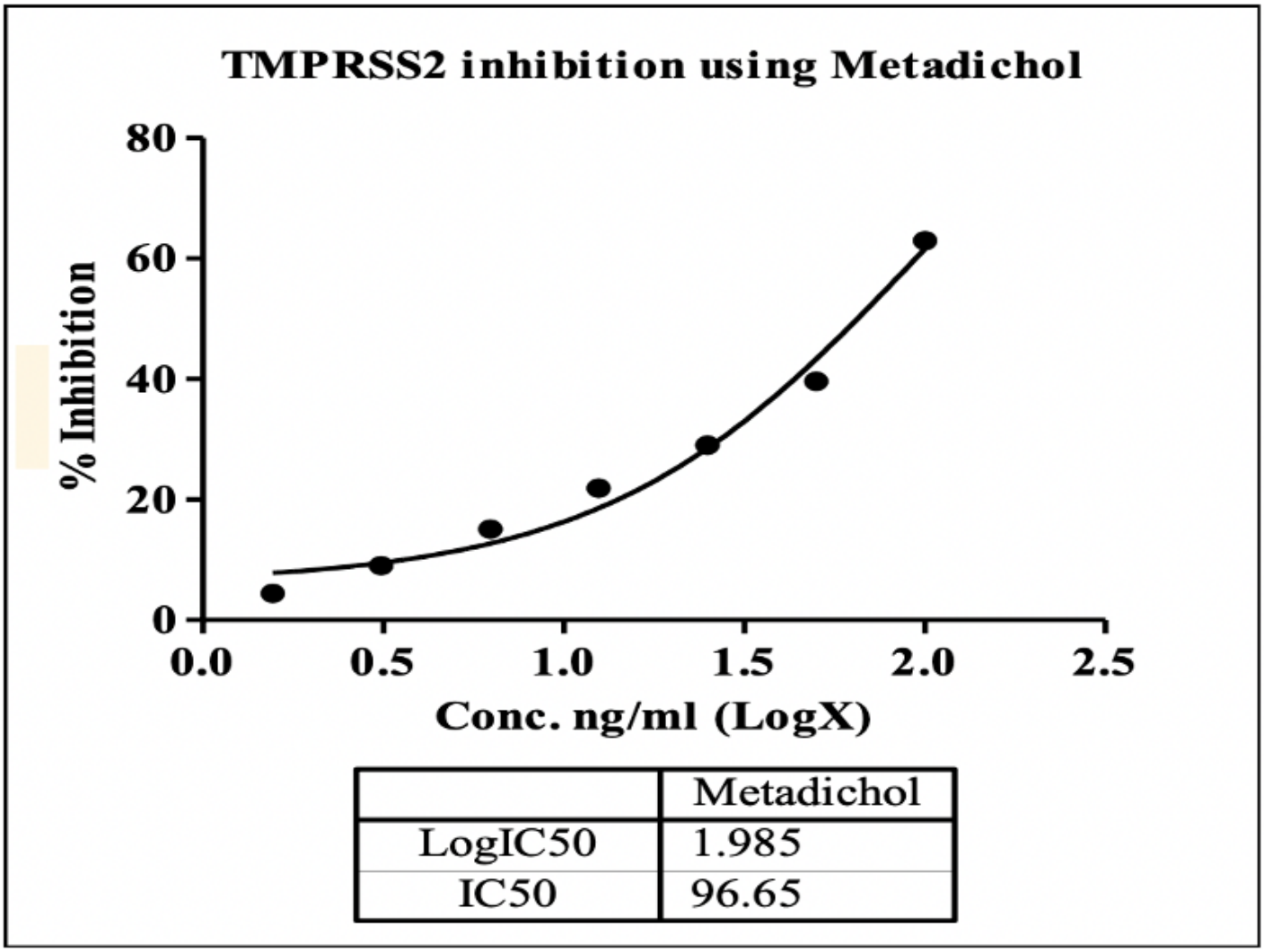

Figure 2

TMPRSS2 inhibition with Metadichol

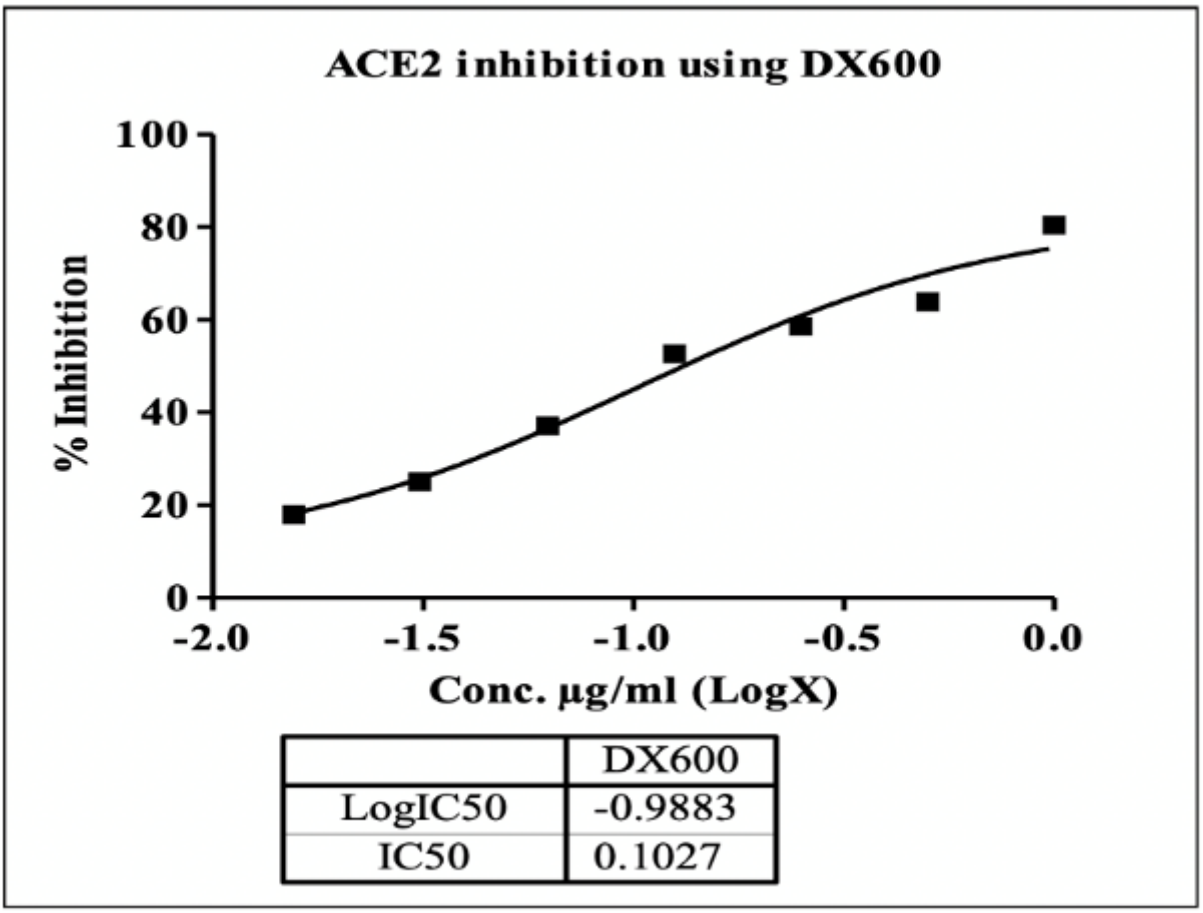

Figure 3

Ace-2 inhibition and DX 600 (control)

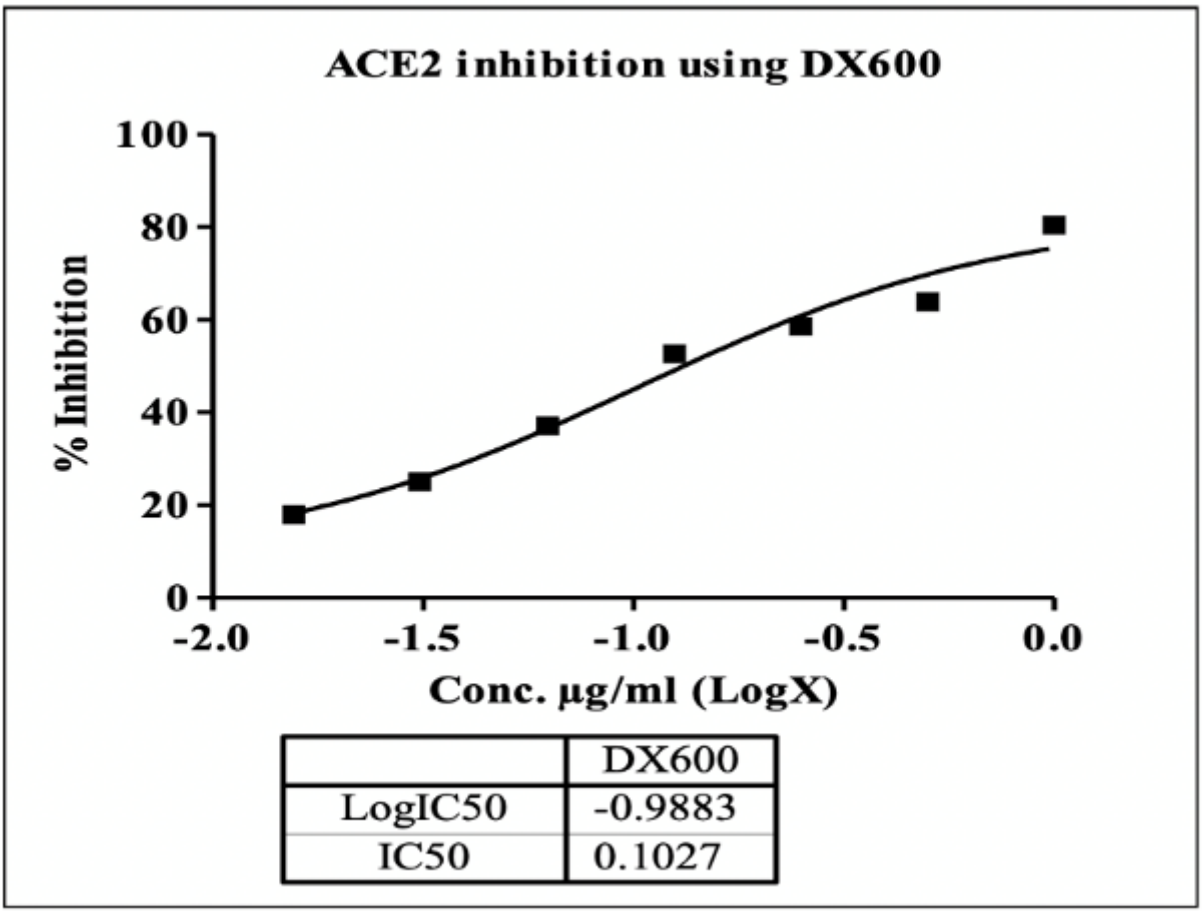

Figure 3

Ace-2 inhibition and DX 600 (control)

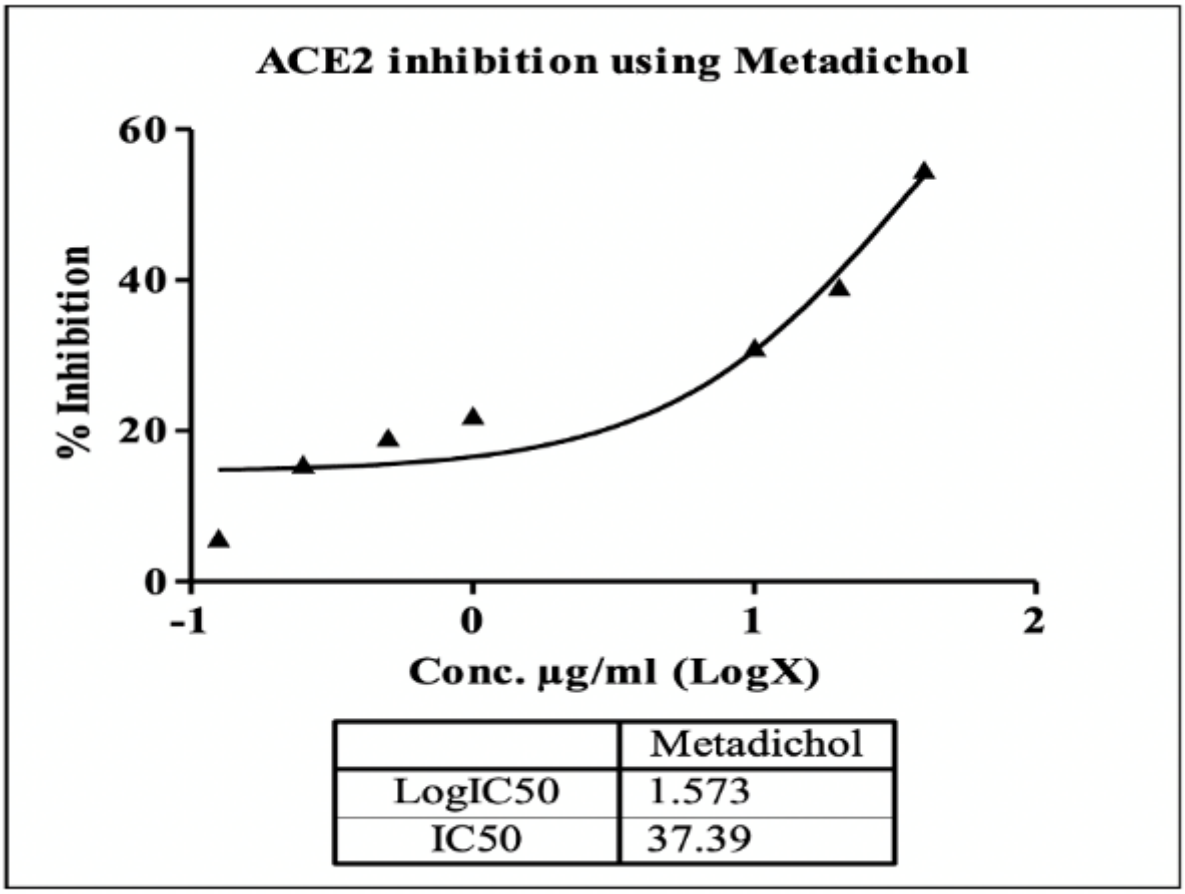

	Metadichol
LogIC50	1.573
IC50	37.39

Figure 4

ACE2 inhibition with Metadichol

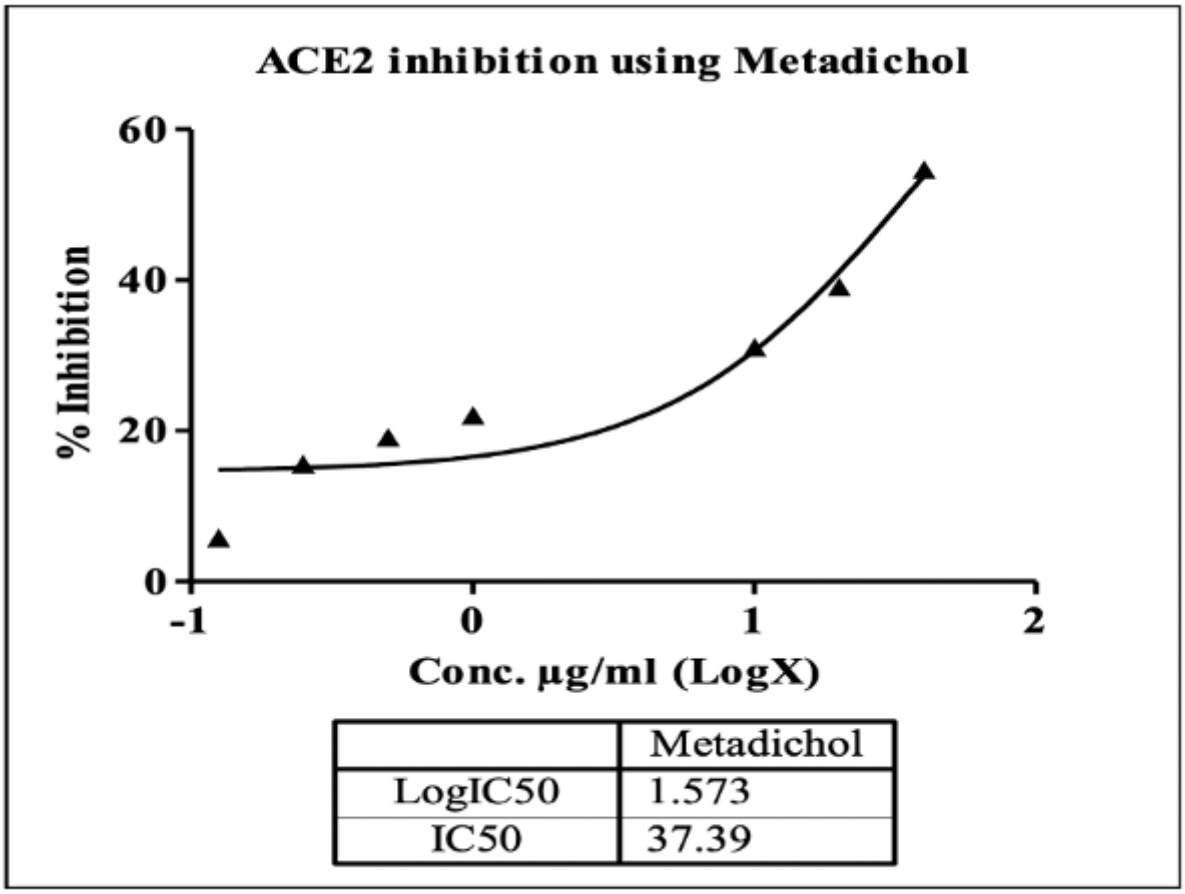

	Metadichol
LogIC50	1.573
IC50	37.39

Figure 4

ACE2 inhibition with Metadichol

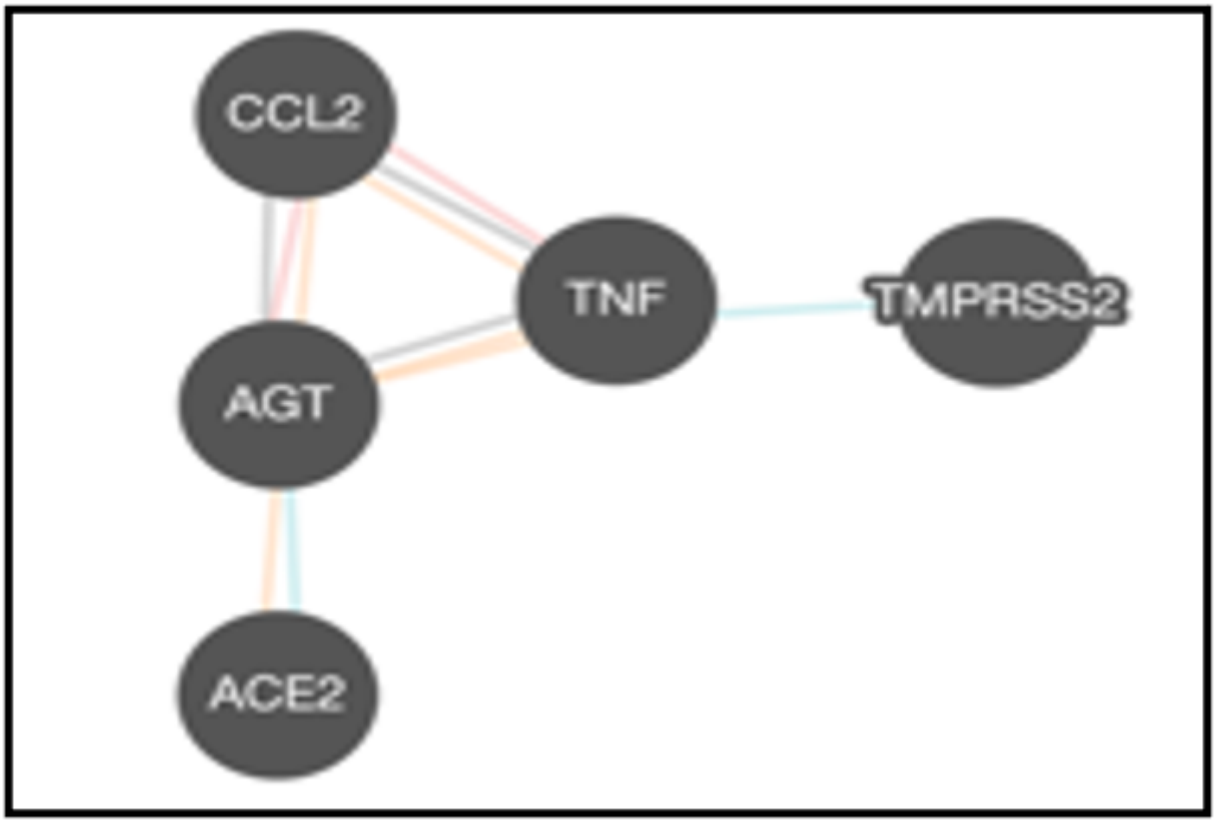

Figure 5

Potential key gene targets in SARS-COV-2 infection

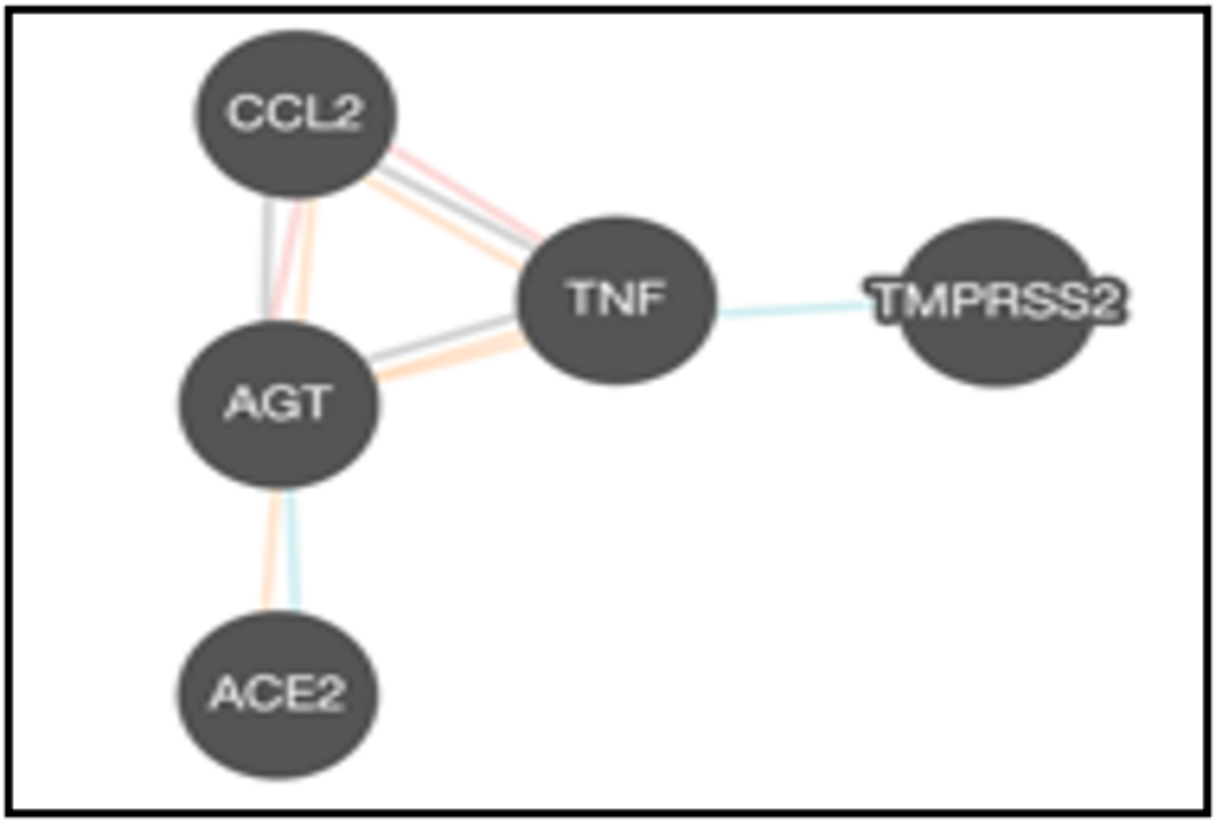

Figure 5

Potential key gene targets in SARS-COV-2 infection

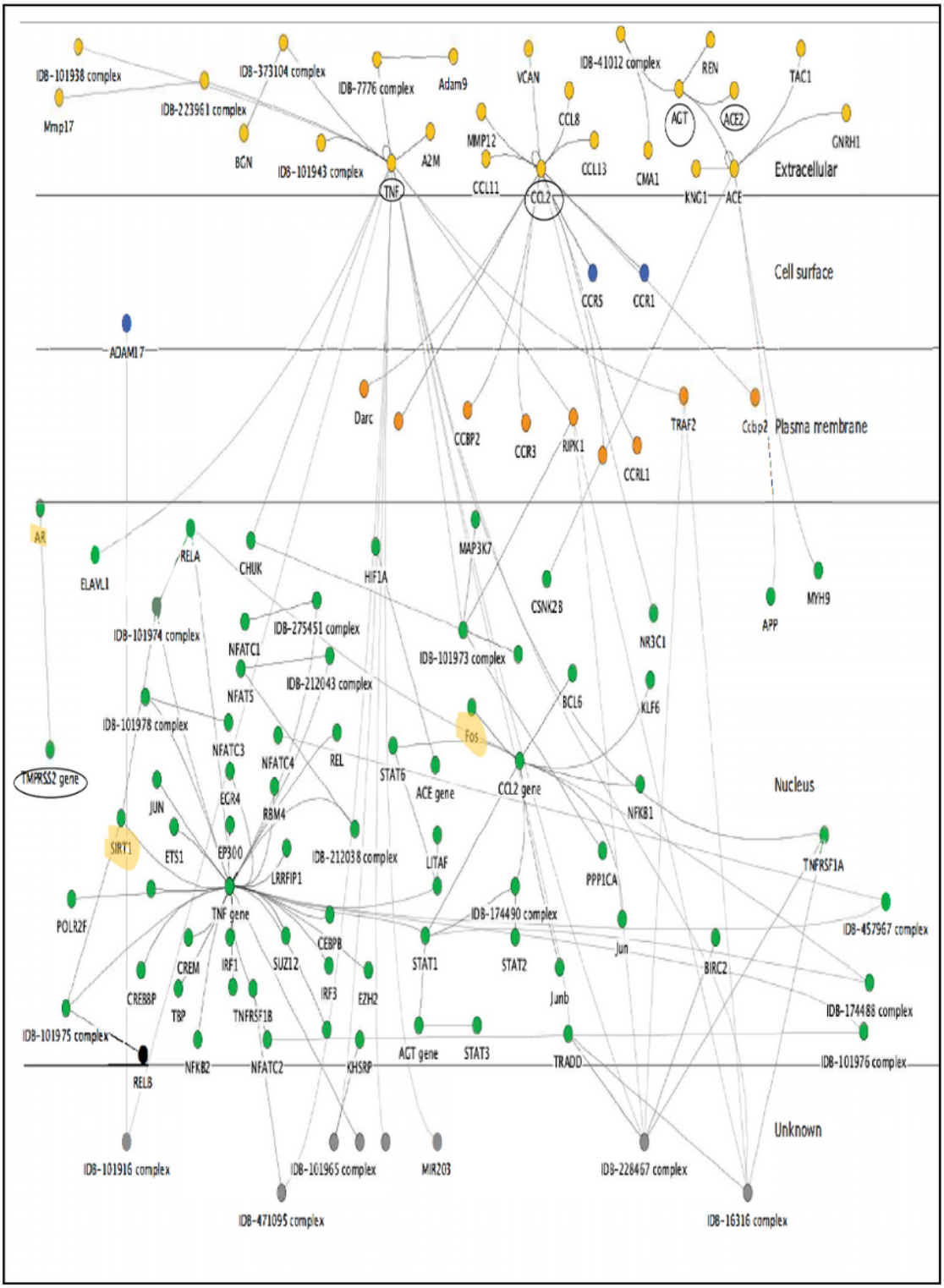

Figure 6

Network analysis of genes involved in SARS-COV-2 infections

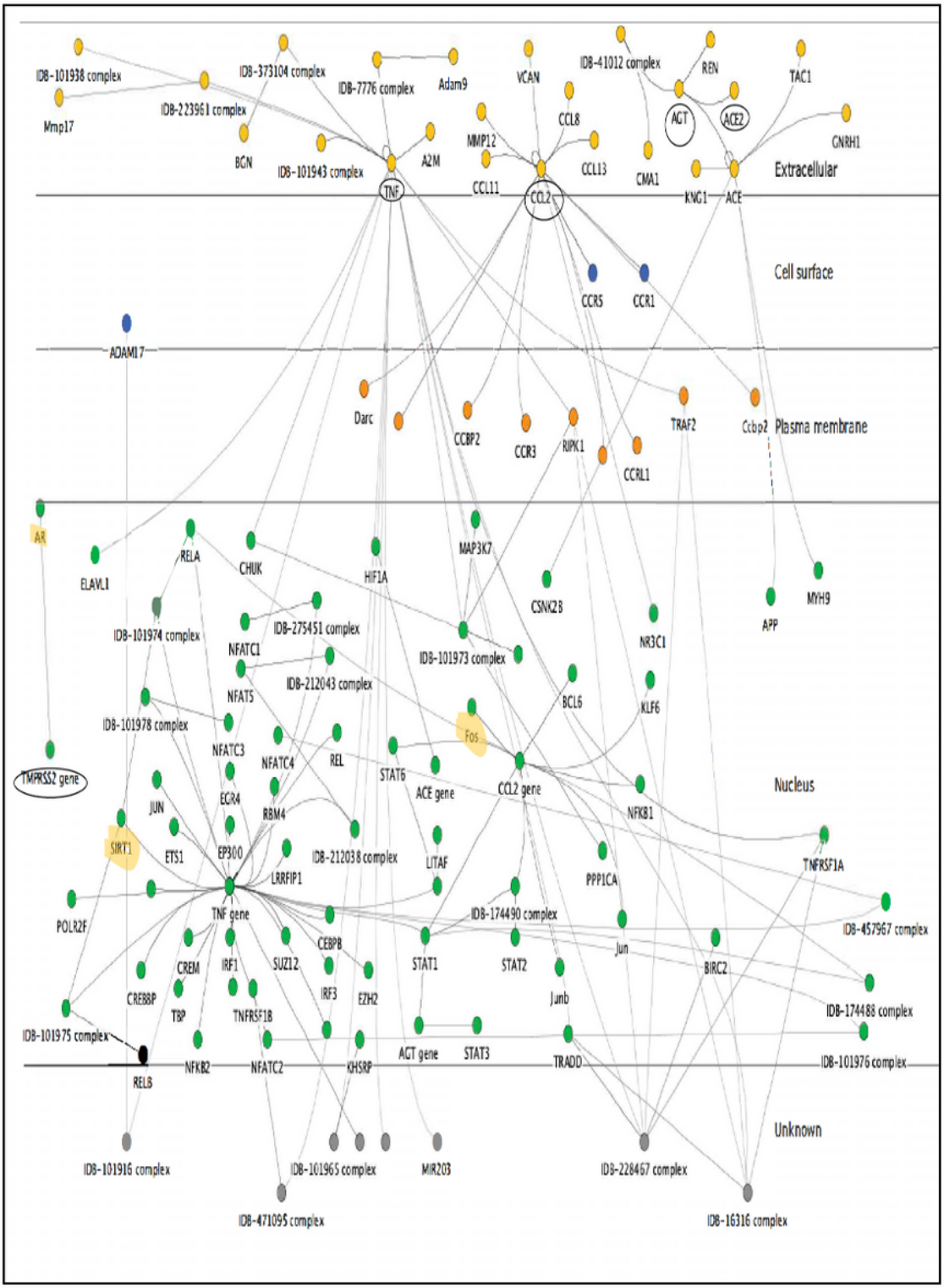

Figure 6

Network analysis of genes involved in SARS-COV-2 infections

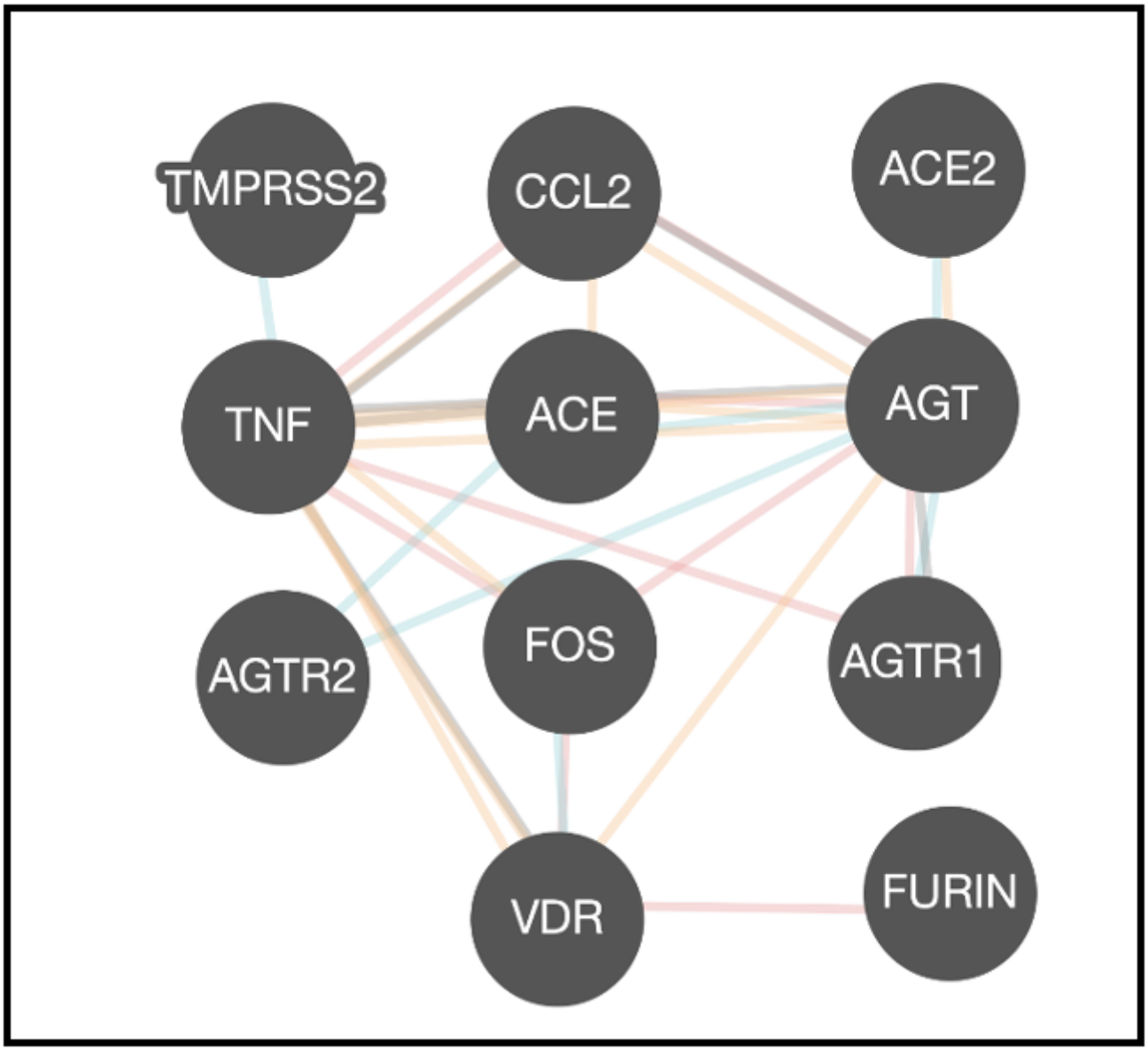

Figure 7

Cytokine relationship and network

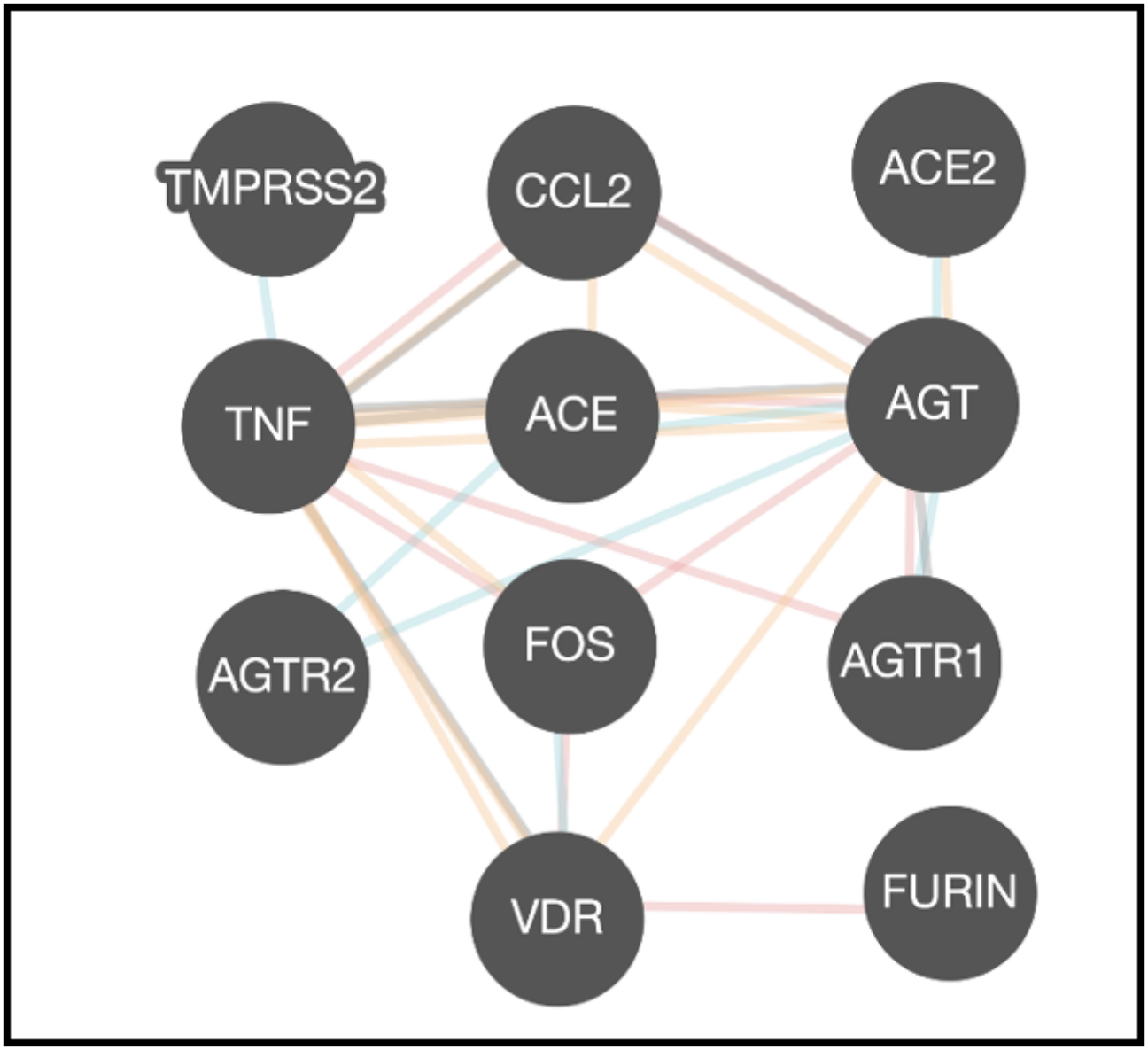

Figure 7

Cytokine relationship and network

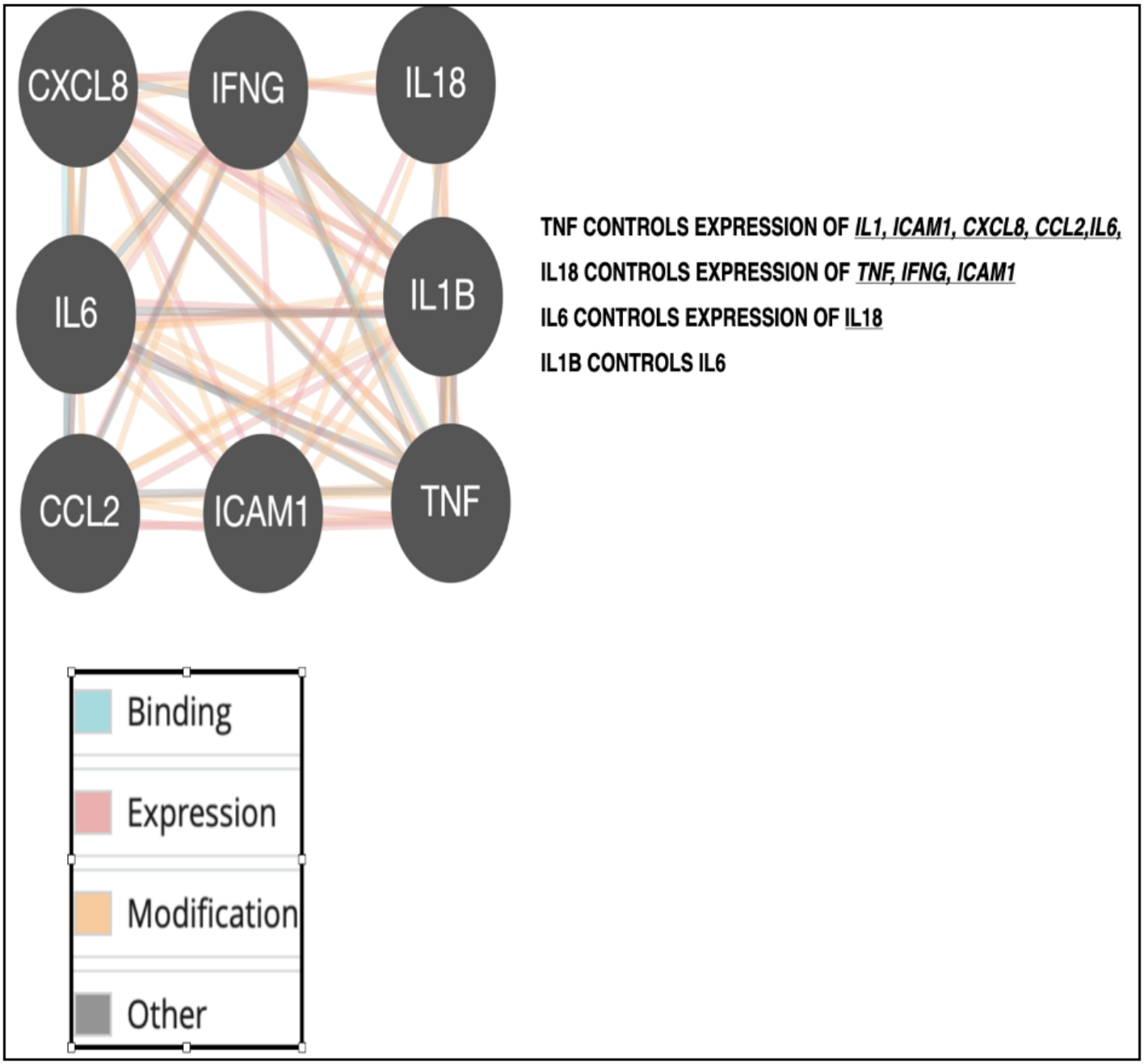

Figure 8

RAS- and VDR- gene relationships

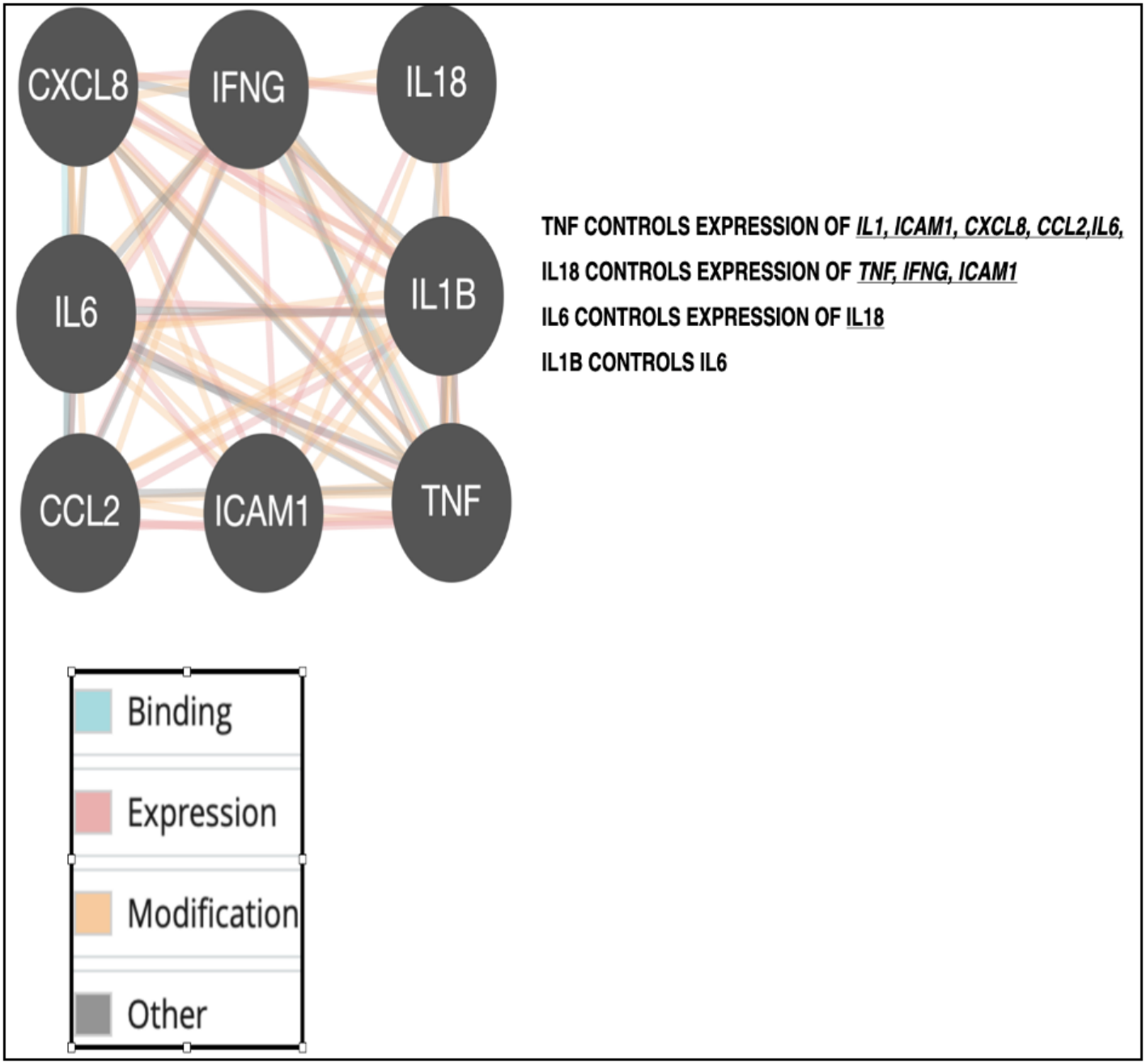

Figure 8

RAS- and VDR- gene relationships

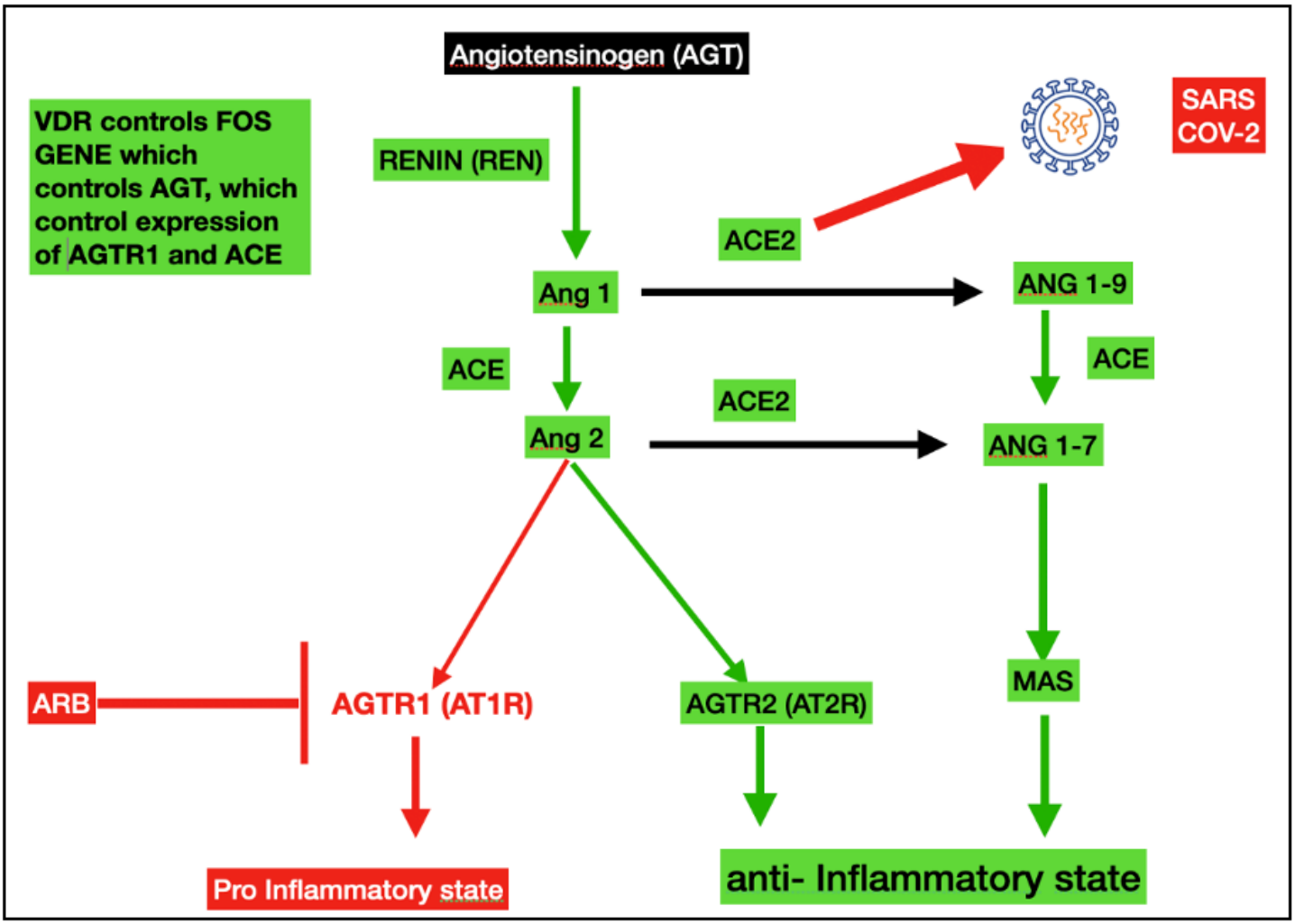

Figure 9

RAS and VDR

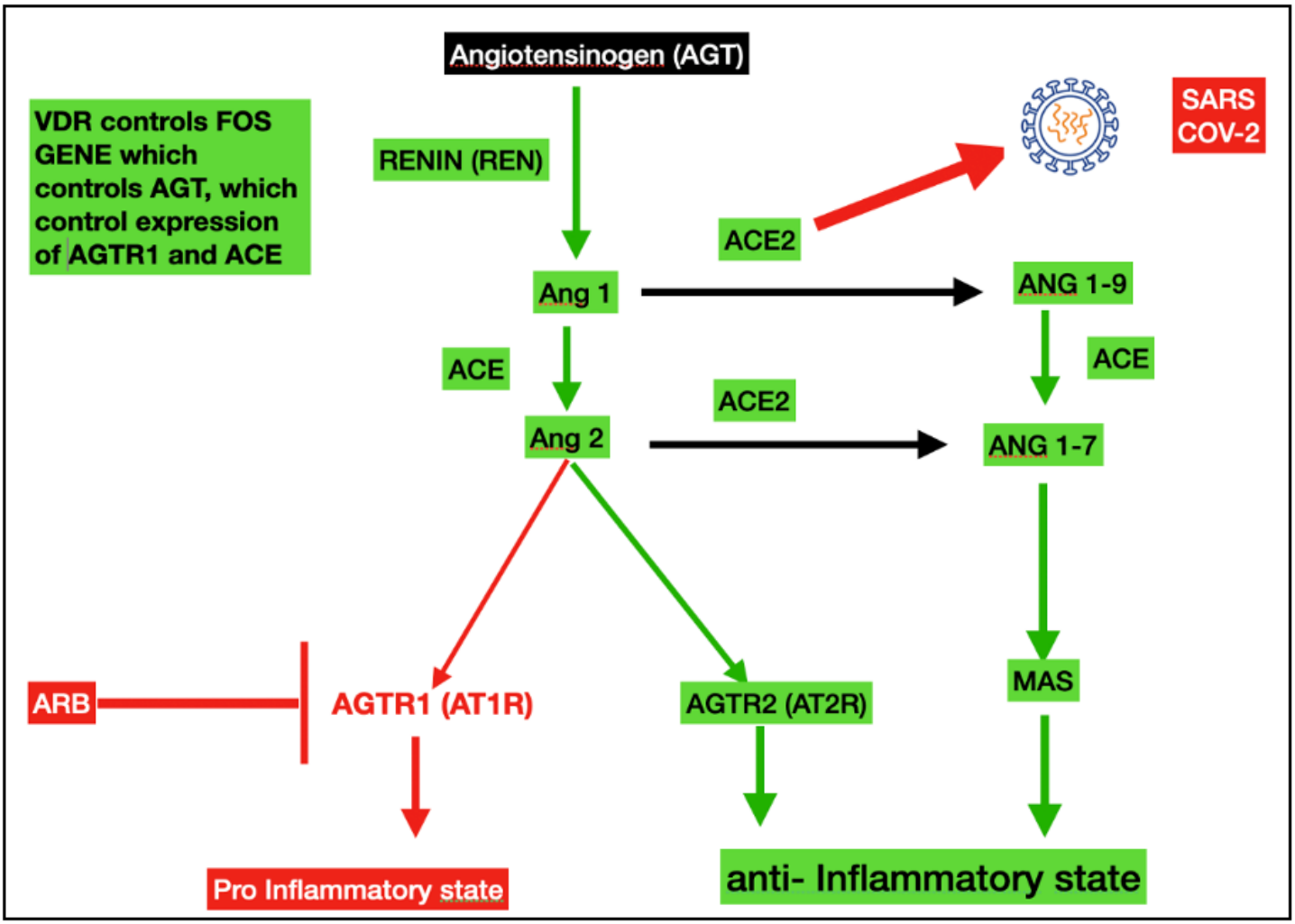

Figure 9

RAS and VDR